Numerische Mathematik manuscript No.
(will be inserted by the editor)

Runge–Kutta physics informed neural networks: formulation and analysis

Georgios Akrivis · Charalambos G. Makridakis · Costas Smaragdakis

Received: 17 January 2025 / Accepted: 4 September 2025

Abstract In this paper we consider time-dependent PDEs discretized by a special class of Physics Informed Neural Networks whose design is based on the framework of Runge–Kutta and related time-Galerkin discretizations. The primary motivation for using such methods is that alternative time-discrete schemes not only enable higher-order approximations but also have a crucial impact on the *qualitative behavior* of the discrete solutions. The design of the methods follows a novel training approach based on two key principles: (a) *the discrete loss is designed using a time-discrete framework*, and (b) *the final loss formulation incorporates Runge–Kutta or time-Galerkin discretization* in a carefully structured manner. We then demonstrate that the resulting methods inherit the stability properties of the Runge–Kutta or time-Galerkin schemes, and furthermore, their computational behavior aligns with that of the original time discrete method used in their formulation. In our analysis, we focus on linear parabolic equations, demonstrating both the stability of the methods and the convergence of the discrete minimizers to solutions of the underlying evolution PDE. An important novel aspect of our work is the derivation of

G. Akrivis
Department of Computer Science and Engineering, University of Ioannina, 451 10 Ioannina, Greece, and Institute of Applied and Computational Mathematics, FORTH, 700 13 Heraklion, Crete, Greece.
E-mail: akrivis@cse.uoi.gr

Ch. G. Makridakis
Modeling and Scientific Computing, Department of Mathematics & Applied Mathematics, University of Crete / Institute of Applied and Computational Mathematics, FORTH, 700 13 Heraklion, Crete, Greece, and MPS, University of Sussex, Brighton BN1 9QH, United Kingdom.
E-mail: C.G.Makridakis@iacm.forth.gr

C. Smaragdakis
Department of Statistics and Actuarial-Financial Mathematics, University of the Aegean, 832 00, Karlovassi, Greece, and Institute of Applied and Computational Mathematics, FORTH, 700 13 Heraklion, Crete, Greece.
E-mail: kesmarag@aegean.gr

maximal regularity (MR) estimates for B-stable Runge–Kutta schemes and both continuous and discontinuous Galerkin time discretizations. This allows us to provide new energy-based proofs for maximal regularity estimates previously established by Kovács, Li, and Lubich [30], now in the Hilbert space setting and with the flexibility of variable time steps.

Keywords Physics informed neural networks · Runge–Kutta methods · collocation methods · Galerkin time-stepping methods · maximal parabolic regularity

Mathematics Subject Classification (2000) 65M15 · 68T01 · 68T07

1 Introduction

1.1 Evolutionary PDEs and Neural Network Discretizations

In this paper, we consider time-dependent PDEs discretized by a special class of Physics Informed Neural Networks whose design is based on the framework of Runge–Kutta and related time-Galerkin discretizations. The key motivation for adopting such methods lies in their ability not only to achieve higher-order approximations but also to significantly influence the *qualitative behavior* of the discrete solutions. These physically consistent approximations are critical for numerous applications, as underscored by the rich and significant literature on time-discrete methods in numerical analysis and scientific computation; see, e.g., [11], [15], [16], [12], [10], [26], [27], [49]. Characteristic examples include conservative schemes for wave and Schrödinger equations, dissipative schemes for diffusion equations preserving the smoothing effect of the equation, geometry and structure preserving schemes, and specially tuned time discretizations for the Navier–Stokes equations.

Formulation of the RK-PINN methods

Physics Informed Neural Networks are algorithms where the discretization is based on the minimization of the L^2 norm of the residual of the evolution PDE over a set of neural networks with a given architecture. Computing the loss requires an additional quadrature step to evaluate the space-time integrals, a process known as *training*. Standard approaches, particularly in high dimensions, often rely on probabilistic quadrature methods like Monte Carlo or Quasi-Monte Carlo. However, the impact of these discrete losses on the qualitative behavior of the approximations remains largely unexplored. Notably, even for the scalar wave equation, we lack clarity on whether and under what conditions these methods preserve key conservation properties.

In this work, we propose a novel training approach based on two key principles:

(a) *the discrete loss is designed using a time-discrete framework*, and

(b) *the final loss formulation incorporates Runge–Kutta or time-Galerkin discretization* in a carefully structured manner.

We then demonstrate that the resulting methods inherit the stability properties of the Runge–Kutta or time-Galerkin schemes, and furthermore, their computational behavior aligns with that of the original time discrete method used in their formulation. Since time-discrete training affects only the time variable, the resulting schemes are particularly well-suited for high-dimensional evolution problems.

Analysis through novel Maximal Regularity estimates

In our analysis, we focus on linear parabolic equations, demonstrating both the stability of the methods and the convergence of the discrete minimizers to solutions of the underlying evolution PDE. Following the approach in [21], we employ the liminf-limsup framework of De Giorgi (see Section 2.3.4 of [17] and [9]), which is widely used in the Γ-convergence of functionals for nonlinear PDEs.

We first establish that the proposed methods yield stable functionals in the sense of properties [S1] and [S2], as defined in Section 3.1.1. Our analysis reveals that stability is rooted in strong discrete regularity estimates associated with maximal regularity. A key novel contribution of our work is the derivation of maximal regularity (MR) estimates for B-stable Runge–Kutta schemes, as well as for both continuous and discontinuous Galerkin time discretizations. This allows us to provide new energy-based proofs for maximal regularity estimates previously established by [30], now in the Hilbert space setting and with the flexibility of variable time steps. This generalizes the results of [30], where constant time steps were a key assumption. See also [33], [2], [28]. An additional interesting feature of our approach is the derivation of the first maximal regularity estimates for high-order Lobatto IIIA methods.

Plan of the paper

In Section 2 we systematically formulate the methods considered in this work. To motivate our approach, we use as a model a linear parabolic equation, but the algorithms are clearly applicable to a wide selection of evolution equations. First, we consider simple time discrete training methods and then we employ the pointwise formulation of [3] to design the various Runge–Kutta Physics Informed Neural Networks (RK-PINNs).

Section 3 is devoted to the analysis of the methods in the case of linear parabolic equations by establishing that the neural network approximations satisfy crucial properties related to the liminf-limsup framework mentioned above, [17]. To prove stability, Proposition 3.1, we rely on maximal regularity estimates. Our novel maximal regularity estimates for Runge–Kutta and both continuous and discontinuous Galerkin time discretizations are assumed

in Section 3 and are systematically derived in Section 4. Theorem 3.1 demonstrates that the sequence of neural network minimizers converges to the exact solution of the parabolic equation, i.e.,

$$\hat{u}_\ell \to u, \quad \text{in } L^2((0,T);H^1(\Omega));$$

see Theorem 3.1 for the precise statement. Throughout, we assume that the approximability capacity of the discrete neural network spaces is given; specifically, we assume that these spaces can approximate smooth functions as described in (3.4), (3.5), and Remark 3.1.

Section 4 is dedicated to deriving maximal regularity estimates within an abstract framework for evolution equations of parabolic type in a Hilbert space. The results presented in this section are of independent interest, both for their proof techniques and because they hold for variable time steps, unlike the results in [30].

We present all time-discrete methods in a unified point-wise formulation as given in (4.3). In Section 4.3, we focus on Galerkin time-stepping methods, including continuous and discontinuous Galerkin methods. Section 4.4 addresses collocation Runge–Kutta methods, with detailed proofs provided for Gauss and Radau IIA methods, as well as for all algebraically stable Runge–Kutta methods. Notably, we derive a novel connection of Lobatto IIIA to continuous Galerkin methods and thus we are able to establish its maximal regularity bounds.

It is worth highlighting that Lobatto IIIA methods are high-order extensions of the trapezoidal rule. Despite being A-stable, their coefficient matrix is not invertible, and they lack B-stability. As a result, our maximal regularity estimates appear to be the first in the literature for this significant family of Runge–Kutta methods.

Section 5 is dedicated to numerical experiments. In addition to parabolic equations, we also consider the wave equation. While the convergence theory for hyperbolic equations remains to be developed, the formulation of the methods can be directly applied by expressing the equation as a first-order evolution system in time.

The numerical results indicate that our proposed methods exhibit the desired properties. They achieve higher accuracy and, more importantly, allow for the adaptation of their qualitative characteristics to produce physically relevant approximations. We did not include computations based on explicit Runge–Kutta discretizations. Instead, we refer to [21], where neural network methods utilizing the *explicit Euler* scheme fail to meet the stability criteria [S1] and [S2], resulting in unstable behavior. To regain stability, these methods require the enforcement of standard CFL conditions that link the space and time discretization parameters.

For training in the spatial variable, we employed quasi-Monte Carlo sampling. This was done both for comparison with full (space and time) quasi-Monte Carlo sampling and to underscore that our approach is well-suited for high-dimensional evolution PDEs. Notably, the time discretization introduces

a mesh only in the time variable, making the method particularly effective in high dimensions.

Remarks on bibliography

Physics Informed Neural Networks is a class of neural network based methods to approximate solutions of PDEs, [43]. The loss is based on the residual of the PDE; similar methods were considered in [32], [6], [42], [47], [38]. Different loss functionals leading to various neural network methods for differential equations are considered in [44], [20], [29], [51], [14], [7] [22], [24]. Previous works on the analysis of these methods include [47], [5], [45], [46], [39, 40], [38], [37].

Neural network approximations for evolution equations have been previously studied in [47], [43], [5], [8], [22], and [24]. In the works [47], [43], [5], a global space-time residual-type loss was employed, whereas in [22] and [24], a time-stepping approach based on the backward Euler or Minimizing Movement schemes was adopted. Discrete time models related to Runge–Kutta methods were considered in [43].

As mentioned, our stability and convergence analysis follows the framework introduced in [21], which is motivated by Γ-convergence arguments. In [41], Γ-convergence was employed to analyze deep Ritz methods without considering training. More recently, the $\liminf - \limsup$ framework was utilized in [34] to establish convergence results for global and local discrete minimizers in general machine learning algorithms with probabilistic training. Additionally, this framework was applied in [23] to analyze deep Ritz methods trained with finite element techniques.

2 Motivation and problem formulation

2.1 Model problems and their Machine Learning approximations

We will consider linear evolution PDEs. The formulation of the methods can be applied to parabolic or wave type time dependent equations, linear or nonlinear, and our main focus is on the effect of the time discretization mechanism.

2.2 A linear evolution PDE

To motivate our approach we consider as a model problem a linear parabolic equation. We use the compact notation $\Omega_T = \Omega \times (0, T]$, for some fixed time $T > 0$. We consider the initial and boundary value problem

$$\begin{cases} u_t + Lu = f & \text{in } \Omega_T, \\ u = 0 & \text{on } \partial\Omega \times (0, T], \\ u(\cdot, 0) = u_0 & \text{in } \Omega, \end{cases} \tag{2.1}$$

where $f \in L^2(\Omega_T)$, $u_0 \in H_0^1(\Omega)$, and L is a coercive, self-adjoint, second order elliptic operator. The associated energies used will be the L^2-residuals

$$\mathcal{E}(v) = \int_0^T \int_\Omega |v_t + Lv - f|^2 \mathrm{d}x\, \mathrm{d}t + |v(0) - u_0|_{H^1}^2 \tag{2.2}$$

defined over smooth enough functions and domains Ω. The choice of the H^1 seminorm for the initial condition, $|v(0) - u_0|_{H^1}$, is done in order to obtain a balanced energy which is particularly convenient in the analysis; obviously, other choices are possible.

Nonlinear Spaces generated by Neural Networks

Physics Informed Neural Networks are based on the minimization of the functional $\mathcal{E}$ over a chosen discrete set consisting of neural networks, aiming at approximating u. To fix ideas, we consider functions u_θ defined through neural networks. The construction below is typical, and it is presented for completeness. Our results only depend on the approximation capacity of these functions. A *deep neural network* maps every point $\overline{x} \in \Omega \times [0,T]$ to $u_\theta(\overline{x}) \in \mathbb{R}$, through

$$u_\theta(\overline{x}) = C_L \circ \sigma \circ C_{L-1} \cdots \circ \sigma \circ C_1(\overline{x}) \quad \forall \overline{x} \in \Omega_T. \tag{2.3}$$

Any such map $\mathcal{C}_L$ is defined by the intermediate (hidden) layers C_k, which are affine maps of the form

$$C_k y = W_k y + b_k, \qquad \text{where } W_k \in \mathbb{R}^{d_{k+1},d_k},\ b_k \in \mathbb{R}^{d_{k+1}}, \tag{2.4}$$

where the dimensions d_k may vary with each layer k and $\sigma(y)$ denotes the vector with the same number of components as y, where $\sigma(y)_i = \sigma(y_i)$. The index θ represents collectively all the parameters of the network $\mathcal{C}_L$, namely W_k, b_k, $k = 1, \dots, L$. The set of all networks $\mathcal{C}_L$ with a given structure (fixed $L, d_k, k = 1, \dots, L$) of the form (2.3), (2.4) is called $\mathcal{N}$. The total dimension (total number of degrees of freedom) of $\mathcal{N}$, is $\dim \mathcal{N} = \sum_{k=1}^{L} d_{k+1}(d_k + 1)$. We now define the nonlinear discrete set of functions

$$V_{\mathcal{N}} = \{u_\theta : \Omega_T \to \mathbb{R},\ \text{where } u_\theta(\overline{x}) = \mathcal{C}_L(\overline{x}),\ \text{for some } \mathcal{C}_L \in \mathcal{N}\}. \tag{2.5}$$

Boundary conditions is a subtle issue. To avoid extra technical problems, it will be useful to introduce, following [48], the set of functions which exactly satisfy the boundary conditions through appropriate distance functions depending only on the domain Ω. If Φ is such a function, see [48, Section 5.1.1], we define

$$V_{\mathcal{N},0} = \{u_\theta : \Omega_T \to \mathbb{R},\ \text{where } u_\theta(x,t) = \Phi(x)\mathcal{C}_L(x,t) \text{ for some } \mathcal{C}_L \in \mathcal{N}\}. \tag{2.6}$$

Then, $V_{\mathcal{N},0} \subset H^1((0,T); L^2(\Omega)) \cap L^2((0,T); H^2(\Omega) \cap H_0^1(\Omega))$, for smooth enough activation function σ. It should be noted that the above choice is meaningful only when approximating sufficiently smooth solutions; see [21] for

a detailed analysis of cases where elliptic regularity estimates fail. An alternative and robust approach is to enforce the boundary conditions via Lagrange multipliers, combined with corresponding Uzawa algorithms, [37].

Abstract Loss – minimization on $V_{\mathcal{N}}$

Physics Informed Neural networks are based on the minimization of residual-type functionals of the form (2.2) over discrete neural network sets of given architecture. To this end, we assume that the (non-computable) abstract problem

$$\min_{v \in V_{\mathcal{N},0}} \mathcal{E}(v) \tag{2.7}$$

possesses a solution $v^\star \in V_{\mathcal{N},0}$. The integrals appearing in the loss functional $\mathcal{E}$ require further discretization to result in a computable loss. As the set $V_{\mathcal{N},0}$ is nonlinear, the problem needs to be considered as minimization in the parameter space over $\mathbb{R}^{\dim \mathcal{N}}$

$$\min_{\theta \in \Theta} \mathcal{E}(u_\theta), \tag{2.8}$$

which turns out to be non-convex with respect to θ even though the functional $\mathcal{E}(v)$ is convex with respect to v.

2.3 Simple time-discrete Training

To formulate fully discrete schemes, we shall need computable discrete versions of the energy $\mathcal{E}(u_\theta)$. This can be achieved through deterministic or probabilistic training.

Deterministic and probabilistic training

We consider appropriate quadrature for integrals over Ω_T (Training through quadrature). Such a quadrature requires a set K_h of discrete points $z \in K_h$ and corresponding nonnegative weights w_z such that

$$\sum_{z \in K_h} w_z g(z) \approx \int_{\Omega_T} g(\overline{x})\, \mathrm{d}\overline{x}. \tag{2.9}$$

Then, one can define the discrete functional

$$\mathcal{E}_{Q,h}(g) = \sum_{z \in K_h} w_z |v_t(z) + Lv(z) - f(z)|^2. \tag{2.10}$$

The initial condition is discretized in a similar way.

An alternative is to approximate integrals using probabilistic (Monte Carlo, Quasi-Monte Carlo) quadrature rules. To this end, we may consider a collection $X_1, X_2, \dots$ of i.i.d. Ω_T-valued random variables, defined on an appropriate

probability space corresponding to sample points in Ω_T. Let ω be a fixed instance, and $X_i(\omega) \in \Omega_T$ be the corresponding values of the random variables. Monte Carlo approximation of the space-time integral yields the discrete sum

$$\mathcal{E}_{N,\omega}(v) = \frac{1}{N}\sum_{i=1}^{N} |v_t(X_i(\omega)) + Lv(X_i(\omega)) - f(X_i(\omega))|^2. \tag{2.11}$$

The discrete minimization problem for each instance is

$$\min_{v\in V_{\mathcal{N},0}} \mathcal{E}_{N,\omega}(v) + \mathcal{E}^0_{N,\omega}(v), \tag{2.12}$$

where $\mathcal{E}^0_{N,\omega}(v)$ is a Monte Carlo approximation of the initial condition. One of the main advantages of these discretizations is that they scale reasonably with the dimension, and are thus preferable for high-dimensional operators L.

Time discrete training

To introduce the Runge–Kutta PINN algorithms, it will be instrumental to consider a hybrid approach where quadrature (and discretization) is applied only to the time variable of the time dependent problem. Then, the fully discrete scheme can be designed using alternative discretizations in space, deterministic or probabilistic.

To fix notation, let $0 = t_0 < t_1 < \cdots < t_N = T$ define a partition of $[0,T]$ and $J_n := (t_n, t_{n+1}]$, $k_n := t_{n+1} - t_n$. We denote by $v_m(\cdot)$ and $f_m(\cdot)$ the values $v(\cdot, t_m)$ and $f(\cdot, t_m)$. Then, we consider the discrete in time quadrature

$$\sum_{n=0}^{N-1} k_n\, g(t_{n+1}) \approx \int_0^T g(t)\,\mathrm{d}t. \tag{2.13}$$

We proceed to define the time-discrete version of the functional (2.2) as follows

$$\begin{aligned}\mathcal{G}_{k,IE}(v) = \sum_{n=0}^{N-1} k_n \int_\Omega \left|\frac{v_{n+1}-v_n}{k_n} + Lv_{n+1} - f(t_{n+1})\right|^2 \mathrm{d}x \\ + |v_0 - u_0|^2_{H^1(\Omega)}.\end{aligned} \tag{2.14}$$

In [21], it was shown that the problem

$$\min_{v\in V_{\mathcal{N}}} \mathcal{G}_{k,IE}(v) \tag{2.15}$$

yields stable and convergent approximations to the exact solution as opposed to the analogue (from the point of view of quadrature and approximation) discrete functional:

$$\mathcal{G}_{k,EE}(v) = \sum_{n=0}^{N-1} k_n \int_\Omega \left|\frac{v_{n+1}-v_n}{k_n} + Lv_n - f(t_n)\right|^2 \mathrm{d}x + |v_0 - u_0|^2_{H^1(\Omega)}. \tag{2.16}$$

Thereby hinting that there is a deeper connection between standard stability notions of time discretizations and this class of neural network algorithms. In the analysis, it was instrumental to consider an alternative representation of the time discrete functional through reconstructions. This can motivate the design of the Runge–Kutta PINN methods of the next section. Indeed, let the *linear time reconstruction* $\widehat{v}$ of a time dependent function v be the piecewise linear approximation of v defined by linearly interpolating between the nodal values v_n and v_{n+1}:

$$\widehat{v}(t) := \ell_0^n(t)v_n + \ell_1^n(t)v_{n+1}, \quad t \in J_n, \tag{2.17}$$

with $\ell_0^n(t) := (t_{n+1} - t)/k_n$ and $\ell_1^n(t) := (t - t_n)/k_n$. If the piecewise constant interpolant of v_j is denoted by $\overline{v}$,

$$\overline{v}(t) := v_{n+1}, \quad t \in J_n\,, \tag{2.18}$$

the time discrete energy $\mathcal{G}_{k,IE}$ becomes

$$\begin{aligned} \mathcal{G}_{k,IE}(v) &= \|\widehat{v}_t + L\overline{v} - \overline{f}\|^2_{L^2((0,T);L^2(\Omega))} + |\widehat{v}(0) - u_0|^2_{H^1(\Omega)} \\ &= \int_0^T \|\widehat{v}_t + L\overline{v} - \overline{f}\|^2_{L^2(\Omega)}\,\mathrm{d}t + |\widehat{v}(0) - u_0|^2_{H^1(\Omega)}. \end{aligned} \tag{2.19}$$

This representation of the loss will be generalized to high-order time discretizations in the next section.

2.4 Runge–Kutta Physics Informed Neural Networks

To introduce the Runge–Kutta PINNs, we first recall the connection of Runge–Kutta methods and collocation time discretizations.

2.4.1 Collocation Runge–Kutta methods

For $q \in \mathbb{N}$, let $0 \leqslant c_1 < \cdots < c_q \leqslant 1$ denote the intermediate nodes of a Runge–Kutta method or collocation nodes. With starting value $U_0 = u_0$, we consider the discretization of problem (2.1) by a q-stage Runge–Kutta method: we recursively define approximations $U_\ell \in V$ to the nodal values $u(t_\ell)$, as well as internal approximations $U_{\ell i} \in V$ to the intermediate values $u(t_{\ell i}), t_{\ell i} = t_\ell + c_i k_\ell$, by

$$\begin{cases} U_{ni} = U_n - k_n \sum_{j=1}^{q} a_{ij}\big(LU_{nj} - f(t_{nj})\big), \quad i = 1, \dots, q, \\ U_{n+1} = U_n - k_n \sum_{i=1}^{q} b_i\big(LU_{ni} - f(t_{ni})\big), \end{cases} \tag{2.20}$$

$n = 0, \dots, N-1$. Here, without being very precise, V is a functional space where our approximations are sought for every $t \in [0,T]$; typically V is included in the domain of the operator L. The most important class of Runge–Kutta methods are the *collocation Runge–Kutta* methods, [25], [50], [26]. Such methods are equivalent to considering a collocation approximation $\widehat{U}$ which is a continuous piecewise polynomial function of local degree q satisfying $\widehat{U}(0) = u_0$ and the collocation conditions

$$\widehat{U}'(t_{ni}) + L\widehat{U}(t_{ni}) = f(t_{ni}), \quad i = 1, \dots, q, \quad n = 0, \dots, N-1. \tag{2.21}$$

The q-stage Runge–Kutta method and the collocation points are related through the relations

$$a_{ij} = \int_0^{c_i} \ell_j(\tau)\,\mathrm{d}\tau, \quad b_i = \int_0^1 \ell_i(\tau)\,\mathrm{d}\tau, \quad i,j = 1, \dots, q; \tag{2.22}$$

here, $\ell_1, \dots, \ell_q \in \mathbb{P}_{q-1}$ are the Lagrange polynomials for the collocation nodes $c_1, \dots, c_q$, $\ell_i(c_j) = \delta_{ij}, i,j = 1, \dots, q$. In this case, the *stage order* of the Runge–Kutta method is q.

It is well known, [25], [50], [26], that the collocation and Runge–Kutta methods (2.21) and (2.20), respectively, are equivalent in the sense that they yield the same approximations at the nodes and at the intermediate nodes, i.e.,

$$\begin{aligned} &\widehat{U}(t_n) = U_n, \qquad n = 1, \dots, N, \\ &\widehat{U}(t_{ni}) = U_{ni}, \quad i = 1, \dots, q, \ \ n = 0, \dots, N-1. \end{aligned} \tag{2.23}$$

These methods admit a crucial pointwise formulation which is the key element of the loss functional defined below. Indeed, as in [3] and [4], if we let I_{q-1} be the piecewise interpolation operator by polynomials of degree $q-1$ at the collocation nodes $t_{ni}, i = 1, \dots, q, n = 0, \dots, N-1$, and because $\widehat{U}'$ is a piecewise polynomial of degree $q-1$ as well, we can write (2.21) in *pointwise form* as

$$\widehat{U}'(t) + LI_{q-1}\widehat{U}(t) = I_{q-1}f(t), \quad t \in (t_n, t_{n+1}], \quad n = 0, \dots, N-1. \tag{2.24}$$

The interpolants $U := I_{q-1}\widehat{U}$ and $I_{q-1}f$ are piecewise polynomials of degree $q-1$ and, in general, discontinuous at the nodes $t_0, \dots, t_{N-1}$. The pointwise form (2.24) of the numerical method will be the basis for defining the Runge–Kutta discrete loss.

2.4.2 Runge–Kutta discrete Loss

We shall introduce more notation related to the representation of piecewise polynomial functions: Let $\ell_{n1}, \dots, \ell_{nq} \in \mathbb{P}_{q-1}$ be the Lagrange polynomials $\ell_1, \dots, \ell_q \in \mathbb{P}_{q-1}$ for the collocation nodes $c_1, \dots, c_q$ shifted to the interval $[t_n, t_{n+1}]$, $\ell_{ni}(t) = \ell_{ni}(t_n + k_n\tau) = \ell_i(\tau), i = 1, \dots, q$. Obviously,

$$\ell_{ni}(t_{nj}) = \delta_{ij}, \quad i,j = 1, \dots, q.$$

Furthermore, we let $0 = \tilde{c}_0 < \cdots < \tilde{c}_q = 1$ be auxiliary points, such that $\tilde{c}_0 = 0$ and $\tilde{c}_q = 1$, and let $\tilde{\ell}_{n0}, \tilde{\ell}_{n1}, \ldots, \tilde{\ell}_{nq} \in \mathbb{P}_q$ be the Lagrange polynomials

$$\tilde{\ell}_0, \tilde{\ell}_1 \ldots, \tilde{\ell}_q \in \mathbb{P}_q$$

for the points $\tilde{c}_0, \ldots, \tilde{c}_q$ shifted to the interval $[t_n, t_{n+1}], \tilde{\ell}_{ni}(t) = \tilde{\ell}_{ni}(t_n + k_n\tau) = \tilde{\ell}_i(\tau), i = 0, \ldots, q$. Obviously, $\tilde{\ell}_{ni}(\tilde{t}_{nj}) = \delta_{ij}, i, j = 0, 1, \ldots, q$, with $\tilde{t}_{nj} := t_n + k_n\tilde{c}_j, j = 0, \ldots, q$. With this notation, let the *interpolant* $\widehat{v}$ of a time dependent function v be the piecewise polynomial function approximating v defined by interpolating the nodal values $v(\tilde{t}_{nj})$ of v as follows

$$\widehat{v}(t) = \widehat{I}_q v(t) = \sum_{i=0}^{q} \tilde{\ell}_{ni}(t) v(\tilde{t}_{ni}), \quad \overline{v}(t) = I_{q-1}\widehat{v}(t) = \sum_{j=1}^{q} \ell_{nj}(t)\widehat{v}(t_{nj}), \tag{2.25}$$

for $t \in (t_n, t_{n+1}]$.

Notice that in principle $\tilde{t}_{nj}$ could be different from t_{nj}, and we can choose them at our convenience. The reason of introducing $\tilde{t}_{nj}$ is that we would like to interpolate neural network functions v on the space of *continuous* piecewise polynomial functions and apply afterwards the collocation residual to $\widehat{v}$. In some important cases $\tilde{t}_{nj}$ can be chosen as extensions of the collocation points t_{nj} by including an additional node; see Remark 3.2.

We are ready to define the Runge–Kutta discrete loss by

$$\begin{aligned} \mathcal{G}_{RK}(v) &= \|\widehat{v}_t(t) + LI_{q-1}\widehat{v}(t) - I_{q-1}f(t)\|^2_{L^2((0,T);L^2(\Omega))} + |\widehat{v}(0) - u_0|^2_{H^1(\Omega)} \\ &= \int_0^T \|\widehat{v}_t(t) + LI_{q-1}\widehat{v}(t) - I_{q-1}f(t)\|^2_{L^2(\Omega)}\,\mathrm{d}t + |\widehat{v}(0) - u_0|^2_{H^1(\Omega)}. \end{aligned} \tag{2.26}$$

The Runge–Kutta Physics Informed Neural Network method is based on the discrete minimization problem for the loss $\mathcal{G}_{RK}(v)$,

$$\min_{v \in V_{\mathcal{N},0}} \mathcal{G}_{RK}(v). \tag{2.27}$$

The formulation of the method for nonlinear evolution problems is straightforward by using similar interpolation operators; see [3].

2.4.3 A general discrete Loss

The Runge–Kutta time discretizations as well as continuous and discontinuous time-Galerkin schemes can be cast into a unified formulation showing that the proposed time discrete training can be quite general. This formulation shall be used in the analysis of Sections 3 and 4. We consider generalized interpolation operators as follows: For $q \in \mathbb{N}$, we consider projection or interpolation operators $\mathit{\Pi}_{q-1}, \widetilde{\mathit{\Pi}}_{q-1}$ to the piecewise polynomial functions of local degree $q-1$. Furthermore, we consider a projection or interpolation operator

$$\widehat{v} = \widehat{\mathit{\Pi}}_q v$$

of a time dependent function v to be the piecewise polynomial function of local degree q approximating v. We assume that if v is continuous in time, then $\widehat{v}$ is a piecewise polynomial globally continuous in time function. The standard interpolation operators as defined in Section 2.4.2 are typical cases of these operators. We are ready to define the time-discrete loss by

$$\mathcal{G}_k(v) = \int_0^T \|\widehat{v}_t(t) + L\Pi_{q-1}\widehat{v}(t) - \widetilde{\Pi}_{q-1}f(t)\|^2_{L^2(\Omega)}\,\mathrm{d}t + |\widehat{v}(0) - u_0|^2_{H^1(\Omega)}. \tag{2.28}$$

In Section 4 we show systematically that all Runge–Kutta methods considered and both continuous and discontinuous Galerkin time discrete schemes are associated to the general formulation involving the discrete operators Π_{q-1}, $\widetilde{\Pi}_{q-1}$ and $\widehat{\Pi}_q$.

The generalized Runge–Kutta Physics Informed Neural Network method is based on the discrete minimization problem for the loss $\mathcal{G}_k(v)$,

$$\min_{v\in V_{\mathcal{N},0}} \mathcal{G}_k(v). \tag{2.29}$$

Under certain assumptions on the generalized operators (see Proposition 3.1, (3.12), and (3.20)), we conduct the stability and convergence analysis for (2.29) in Section 3. These assumptions are shown to be satisfied by all the methods discussed in this work, as demonstrated in Section 4.

3 Stability and Convergence for Parabolic equations

Let as before $\Omega \subset \mathbb{R}^d$ be open and bounded, and set $\Omega_T = \Omega \times (0, T]$ for some fixed time $T > 0$. We consider the parabolic problem

$$\begin{cases} u_t + Lu = f & \text{in } \Omega_T, \\ u = 0 & \text{on } \partial\Omega \times (0, T], \\ u(\cdot, 0) = u_0 & \text{in } \Omega. \end{cases} \tag{3.1}$$

In this section we discuss convergence properties of approximations of (3.1) obtained by minimization of continuous and time-discrete energy functionals over appropriate sets of neural network functions. We shall assume that Ω is a convex Lipschitz domain. This assumption is made to ensure that elliptic regularity estimates are valid. The case of a non-convex domain can be treated with the appropriate modifications in the analysis.

The continuous functional can be defined as follows: Consider

$$\mathcal{G} : H^1((0,T); L^2(\Omega)) \cap L^2((0,T); H^2(\Omega) \cap H^1_0(\Omega)) \to \overline{\mathbb{R}}$$

such that

$$\mathcal{G}(v) = \int_0^T \|v_t(t) + Lv(t) - f(t)\|^2_{L^2(\Omega)}\mathrm{d}t + |v(0) - u_0|^2_{H^1(\Omega)}. \tag{3.2}$$

The use of the $H^1(\Omega)$ seminorm for the initial condition is more appropriate for stability purposes for parabolic equations. While weaker choices are certainly possible, they would require a modified technical analysis.

3.1 Time discrete training through Runge–Kutta and time Galerkin

We shall work with the general time-discrete loss defined in Section 2.4.3:

$$\mathcal{G}_k(v) = \int_0^T \|\widehat{v}_t(t) + L\Pi_{q-1}\widehat{v}(t) - \widetilde{\Pi}_{q-1}f(t)\|^2_{L^2(\Omega)}\,\mathrm{d}t + |\widehat{v}(0) - u_0|^2_{H^1(\Omega)}.$$

In the sequel, we shall use the compact notation

$$\widehat{U} = \widehat{\Pi}_q U, \quad \overline{U} := \Pi_{q-1}\widehat{U}, \quad \text{and} \quad \widetilde{f} = \widetilde{\Pi}_{q-1} f. \tag{3.3}$$

The neural network spaces are selected to meet specific approximability criteria aligned with established results in approximation theory; see, e.g., [1, 18, 51] and their references. However, subtle challenges arise, particularly with boundary conditions and the fact that existing approximation results do not yet offer concrete guidance on selecting specific architectures. Nevertheless, to investigate the potential convergence of minimizers, we assume that the following approximability requirements are satisfied. The required smoothness of the spaces is guaranteed by selecting smooth enough activation functions. The neural network spaces are selected such that for each $\ell \in \mathbb{N}$ we associate a space $V_{\mathcal{N},0}$, which is denoted by V_ℓ with the approximation property: For each $w \in H^1((0,T);L^2(\Omega)) \cap L^2((0,T);H^2(\Omega) \cap H^1_0(\Omega))$ there exists a $w_\ell \in V_\ell$ such that

$$\begin{aligned} &\|w_\ell - w\|_{H^1((0,T);L^2(\Omega))\cap L^2((0,T);H^2(\Omega))} \leqslant \beta_\ell(w), \\ &\text{and } \beta_\ell(w) \to 0, \ \ell \to \infty. \end{aligned} \tag{3.4}$$

If, in addition, w has higher regularity, we assume that

$$\begin{aligned} &\|(w_\ell - w)'\|_{H^1((0,T);L^2(\Omega))\cap L^2((0,T);H^2(\Omega))} \leqslant \tilde{\beta}_\ell \, \|w'\|_{H^m((0,T);H^2(\Omega))}, \\ &\text{and } \tilde{\beta}_\ell \to 0, \ \ell \to \infty, \end{aligned} \tag{3.5}$$

where in the above relation and throughout this section, the time derivative is denoted by w', i.e., $w' := w_t$.

Remark 3.1 The current state of the art in approximating smooth functions using neural network spaces lacks sufficient information regarding the specific architectures necessary to achieve particular bounds and rates. The above assumptions can be relaxed by requiring that (3.4) and (3.5) hold only for $w = u$, where u represents the exact solution of the problem.

With the spaces V_ℓ defined above, we shall use the following notation for the discrete energies:

$$\mathcal{G}_\ell(v_\ell) = \begin{cases} \mathcal{G}_{k(\ell)}(v_\ell), & v_\ell \in V_\ell, \\ +\infty, & \text{otherwise.} \end{cases} \tag{3.6}$$

Here $k = k(\ell)$ are selected just to satisfy $k = k(\ell) \to 0$ as $\ell \to \infty$, and $\mathcal{G}_{k(\ell)}(v_\ell) = \mathcal{G}_k(v_\ell)$ is defined by (3.1).

3.1.1 Stability-Maximal Regularity

Following [21], we call our methods *stable* if two key properties, roughly stated as follows, hold:

[S1] If the energies $\mathcal{E}_\ell$ are uniformly bounded

$$\mathcal{E}_\ell[u_\ell] \leqslant C,$$

then there exists a constant $C_1 > 0$ and ℓ-dependent norms V_ℓ such that

$$\|u_\ell\|_{V_\ell} \leqslant C_1. \tag{3.7}$$

[S2] Uniformly bounded sequences in $\|\cdot\|_{V_\ell}$ have convergent subsequences in H.

Here, H is a normed space (typically a Sobolev space) that depends on the form of the discrete energy being considered. Property [S1] requires that $\mathcal{E}_\ell[v_\ell]$ is coercive with respect to (potentially ℓ-dependent) norms or semi-norms. Moreover, [S2] implies that, although the norms $\|\cdot\|_{V_\ell}$ are ℓ-dependent, they should allow the extraction of convergent subsequences from uniformly bounded sequences in these norms, in a weaker topology induced by the space H.

This definition is inspired by a discrete interpretation of the Equi-Coercivity property in the Γ-convergence framework in the calculus of variations. As we will demonstrate, this property is fundamental to establishing compactness and the convergence of minimizers for the approximate functionals, as shown later in this section.

The stability of $\mathcal{G}_k$ follows by the next result which hinges on the maximal regularity estimates established in Section 4.

Proposition 3.1 *Assume that the following maximal regularity estimate is satisfied*

$$\begin{aligned}\|\overline{U}\|_{L^2((0,T);H^2(\Omega))} + \|\widehat{U}'\|_{L^2((0,T);L^2(\Omega))} \\ \leqslant C\Big[\|\widehat{U}(0)\|_{H^1(\Omega)} + \|\widehat{U}_t + L\overline{U}\|_{L^2((0,T);L^2(\Omega))}\Big];\end{aligned} \tag{3.8}$$

then, the functional $\mathcal{G}_k$ defined in (3.1) is stable with respect to $\widehat{U}, \overline{U}$ in the following sense:

$$\begin{aligned}&\text{If } \mathcal{G}_k(U) \leqslant C \text{ for some } C > 0, \text{ we have} \\ &\|\overline{U}\|_{L^2((0,T);H^2(\Omega))} + \|\widehat{U}'\|_{L^2((0,T);L^2(\Omega))} \leqslant C_{\mathrm{MR}}.\end{aligned} \tag{3.9}$$

Proof Since

$$\int_0^T \|\widehat{U}_t + L\overline{U} - \widetilde{\Pi}_{q-1} f(t)\|^2_{L^2(\Omega)}\,\mathrm{d}t \leqslant C, \tag{3.10}$$

we have

$$\|\widehat{U}_t + L\overline{U}\|_{L^2((0,T);L^2(\Omega))} \leqslant C_1. \tag{3.11}$$

Therefore, in view of (3.8) and the fact that

$$\|\widehat{U}(0)\|_{H^1(\Omega)} \leqslant C$$

as a result of $\mathcal{G}_k(U) \leqslant C$, we conclude the proof.

3.2 Convergence of the minimizers

Next, we shall prove that the sequence of discrete minimizers (u_ℓ) converges in $L^2((0,T);H^1(\Omega))$ to the minimizer of the continuous problem. We first show a lim inf and a lim sup inequality.

Lemma 3.1 (lim inf inequality) *Assume that a sequence $\{U_\ell\}$, $U_\ell \in V_\ell$, satisfies*

$$\mathcal{G}_\ell(U_\ell) \leqslant C$$

uniformly in ℓ. Let the operators $\Pi_{q-1}, \widehat{\Pi}_q$ satisfy

$$\int_{J_n} \widehat{\Pi}_q v \,\mathrm{d}t = \int_{J_n} \Pi_{q-1}\widehat{\Pi}_q v \,\mathrm{d}t\,, \tag{3.12}$$

for all $v \in V_\ell$. Assume further that there exists a $\tilde{u} \in H^1((0,T);L^2(\Omega)) \cap L^2((0,T);H^2(\Omega))$ such that

$$U_\ell \to \tilde{u}, \quad \ell \to \infty, \qquad \text{in } L^2((0,T);H^1(\Omega))\,;$$

then,

$$\mathcal{G}(\tilde{u}) \leqslant \liminf_{\ell\to\infty} \mathcal{G}_\ell(U_\ell). \tag{3.13}$$

Proof From the stability estimate, Proposition 3.1, and the assumption on the boundedness of $\mathcal{G}_\ell(U_\ell)$ we conclude that $\|\overline{U}_\ell\|_{L^2((0,T);H^2(\Omega))} + \|\widehat{U}'_\ell\|_{L^2((0,T);L^2(\Omega))} \leqslant C_1$ are uniformly bounded. By the relative compactness in $L^2((0,T);L^2(\Omega))$ we have (up to a subsequence not re-labeled) the existence of $u_{(1)}$ and $u_{(2)}$ such that

$$L\overline{U}_\ell \rightharpoonup Lu_{(1)} \text{ and } \widehat{U}'_\ell \rightharpoonup u'_{(2)} \text{ weakly in } L^2((0,T);L^2(\Omega))\,. \tag{3.14}$$

Fix a space-time test function $\varphi \in C_0^\infty$, and let I_0 be an appropriate interpolant into the piecewise constants in time functions. Then, (3.12) implies

$$\begin{aligned}
&\Big|\int_0^T (\widehat{U}_\ell, \varphi')\,\mathrm{d}t - \int_0^T (\overline{U}_\ell, \varphi')\,\mathrm{d}t\Big| \\
&\qquad \leqslant \Big|\int_0^T (\widehat{U}_\ell - \overline{U}_\ell, \varphi' - I_0\varphi')\,\mathrm{d}t\Big| + \Big|\int_0^T (\widehat{U}_\ell - \overline{U}_\ell, I_0\varphi')\,\mathrm{d}t\Big| \\
&\qquad = \Big|\int_0^T (\widehat{U}_\ell - \overline{U}_\ell, \varphi' - I_0\varphi')\,\mathrm{d}t\Big|.
\end{aligned} \tag{3.15}$$

By the uniform bound $\|\overline{U}_\ell\|_{L^2((0,T);H^2(\Omega))} + \|\widehat{U}_\ell\|_{L^2(0,T;H^2(\Omega))} \leqslant C_1$, we infer that

$$\int_0^T (\widehat{U}_\ell, \varphi')\,\mathrm{d}t - \int_0^T (\overline{U}_\ell, \varphi')\,\mathrm{d}t \to 0, \quad \ell \to \infty, \tag{3.16}$$

and

$$\int_0^T (L\widehat{U}_\ell, \varphi')\,\mathrm{d}t - \int_0^T (L\overline{U}_\ell, \varphi')\,\mathrm{d}t \to 0, \quad \ell \to \infty. \tag{3.17}$$

We can conclude, therefore, that $u_{(1)} = u_{(2)} = \tilde{u}$, and thus

$$\widehat{U}'_\ell + L\overline{U}_\ell - \overline{f} \rightharpoonup \tilde{u}' + L\tilde{u} - f, \quad \ell \to \infty. \tag{3.18}$$

The convexity of $\int_{\Omega_T} |\cdot|^2$ implies weak lower semicontinuity, that is,

$$\int_{\Omega_T} |\tilde{u}' + L\tilde{u} - f|^2\,\mathrm{d}x\mathrm{d}t \leqslant \liminf_{\ell\to\infty} \int_{\Omega_T} |\widehat{U}'_\ell + L\overline{U}_\ell - \overline{f}|^2\,\mathrm{d}x\mathrm{d}t \tag{3.19}$$

and therefore the proof is complete.

Lemma 3.2 (lim sup **inequality)** *We assume that the operator $\widehat{\Pi}_q$ can be represented as*

$$\widehat{\Pi}_q v(t) = \sum_{i=0}^{q} \tilde{\ell}_{ni}(t) v(\tilde{t}_{ni}), \quad t \in (t_n, t_{n+1}]; \tag{3.20}$$

see (3.20)*. Let $w \in H^1((0,T);L^2(\Omega)) \cap L^2((0,T);H^2(\Omega)\cap H_0^1(\Omega))$. Then, there exists a recovery sequence $\{w_\ell\}$, $w_\ell \in V_\ell$, such that $w_\ell \to w$ and*

$$\mathcal{G}(w) = \lim_{\ell\to\infty} \mathcal{G}_\ell(w_\ell).$$

Proof For $w \in H^1((0,T);L^2(\Omega)) \cap L^2((0,T);H^2(\Omega)\cap H_0^1(\Omega))$, we choose a smooth approximation $(w_\delta) \subset C^\infty([0,T];H^2(\Omega)\cap H_0^1(\Omega))$ such that

$$\begin{aligned} &\|w - w_\delta\|_{H^1((0,T);L^2(\Omega))\cap L^2((0,T);H^2(\Omega))} \lesssim \delta \quad \text{and} \\ &|w'_\delta|_{H^1((0,T);L^2(\Omega))\cap L^2((0,T);H^2(\Omega))} \lesssim \frac{1}{\delta}|w|_{H^1((0,T);L^2(\Omega))\cap L^2((0,T);H^2(\Omega))}. \end{aligned} \tag{3.21}$$

We assign to each δ a discrete function $w_{\delta,\ell} \in V_\ell$ satisfying (3.4) and (3.5). The recovery sequence will be $\{w_{\delta,\ell}\}$, with appropriate $\delta = \delta(\ell)$, and we shall show that

$$\mathcal{G}_{IE,\ell}(w_{\delta,\ell}) \to \mathcal{G}(w)\,. \tag{3.22}$$

We split the error,

$$
\begin{aligned}
&\|\widehat{w}'_{\delta,\ell} + L\,\overline{w}_{\delta,\ell} - w' - Lw\|_{L^2((0,T);L^2(\Omega))} \\
&\qquad \leqslant \|\widehat{w}'_{\delta,\ell} + L\,\overline{w}_{\delta,\ell} - \widehat{w}'_{\delta} - L\,\overline{w}_{\delta}\|_{L^2((0,T);L^2(\Omega))} \\
&\qquad + \|\widehat{w}'_{\delta} + L\,\overline{w}_{\delta} - w'_{\delta} - Lw_{\delta}\|_{L^2((0,T);L^2(\Omega))} \\
&\qquad + \|w'_{\delta} + L\,w_{\delta} - w' - Lw\|_{L^2((0,T);L^2(\Omega))} \\
&\qquad =: A_1 + A_2 + A_3\,.
\end{aligned}
\tag{3.23}
$$

Notice that since $\widehat{\Pi} v(t) = \sum_{i=0}^{q} \tilde{\ell}_{ni}(t) v(\tilde{t}_{ni})$, we have $\sum_{i=0}^{q} \tilde{\ell}_{ni}(t) = 1$ and thus

$$
\sum_{i=0}^{q} \tilde{\ell}'_{ni}(t) = 0
$$

for all n. Hence,

$$
\begin{aligned}
\|\widehat{v}'\|^2_{L^2((0,T);L^2(\Omega))} &= \sum_{n=0}^{N-1} \int_{J_n} \big\|\widehat{v}'\big\|^2_{L^2(\Omega)}\,\mathrm{d}t \\
&= \sum_{n=0}^{N-1} \int_{J_n} \big\| \sum_{i=0}^{q} \tilde{\ell}'_{ni}(t) v(\tilde{t}_{ni})\big\|^2_{L^2(\Omega)}\,\mathrm{d}t \\
&= \sum_{n=0}^{N-1} \int_{J_n} \big\| \sum_{i=1}^{q} \tilde{\ell}'_{ni}(t) (v(\tilde{t}_{ni}) - v(\tilde{t}_{n0})\,)\big\|^2_{L^2(\Omega)}\,\mathrm{d}t \\
&\leqslant \sum_{n=0}^{N-1} \int_{J_n} \sum_{i=1}^{q} \|\tilde{\ell}'_{ni}\|^2_{L^\infty(J_n)} \big\|v(\tilde{t}_{ni}) - v(\tilde{t}_{n0})\big\|^2_{L^2(\Omega)}\,\mathrm{d}t \\
&\leqslant C \sum_{n=0}^{N-1} \frac{1}{k_n} \sum_{i=1}^{q} \big\| \int_{\tilde{t}_{n0}}^{\tilde{t}_{ni}} v'(t)\,\mathrm{d}t\big\|^2_{L^2(\Omega)} \\
&\leqslant C \sum_{n=0}^{N-1} \sum_{i=1}^{q} \int_{\tilde{t}_{n0}}^{\tilde{t}_{ni}} \big\|v'(t)\big\|^2_{L^2(\Omega)}\,\mathrm{d}t \\
&\leqslant C \sum_{n=0}^{N-1} \int_{J_n} \big\|v'(t)\big\|^2_{L^2(\Omega)}\,\mathrm{d}t = C\|v'\|^2_{L^2((0,T);L^2(\Omega))}.
\end{aligned}
\tag{3.24}
$$

Thus, for $\theta_\ell(t) := w_{\delta,\ell}(t) - w_\delta(t)$, we have

$$
\begin{aligned}
\|\widehat{w}'_{\delta,\ell} - \widehat{w}'_{\delta}\|^2_{L^2((0,T);L^2(\Omega))} &= \|\widehat{\theta}'_{\ell}\|^2_{L^2((0,T);L^2(\Omega))} \\
&\leqslant C\|\theta'_{\ell}\|^2_{L^2((0,T);L^2(\Omega))}.
\end{aligned}
\tag{3.25}
$$

Next, we observe that

(3.26)
$$\begin{aligned}
&\|L\overline{w}_{\delta,\ell} - L\overline{w}_\delta\|_{L^2((0,T);L^2(\Omega))} = \Big[\sum_{n=0}^{N-1}\int_{J_n}\big\|L\Pi_{q-1}\theta_\ell\big\|^2_{L^2(\Omega)}\,\mathrm{d}t\Big]^{1/2}\\
&\leqslant \Big[\sum_{n=0}^{N-1}\int_{J_n}\big\|L\Pi_{q-1}\theta_\ell - LP_0\theta_\ell\big\|^2_{L^2(\Omega)}\mathrm{d}t\Big]^{1/2} + \Big[\sum_{n=0}^{N-1}\int_{J_n}\big\|LP_0\theta_\ell\big\|^2_{L^2(\Omega)}\mathrm{d}t\Big]^{1/2}\\
&\leqslant \|L\Pi_{q-1}\theta_\ell - L\theta_\ell\|_{L^2((0,T);L^2(\Omega))} + \|L\theta_\ell - L\,P_0\theta_\ell\|_{L^2((0,T);L^2(\Omega))}\\
&\qquad\qquad + \|L\theta_\ell\|_{L^2((0,T);L^2(\Omega))}\\
&\leqslant Ck\|L\theta'_\ell\|_{L^2((0,T);L^2(\Omega))} + \|L\theta_\ell\|_{L^2((0,T);L^2(\Omega))},
\end{aligned}$$

where we have set $k = \max_n k_n$. We have proved so far that

$$A_1 \leqslant \|\theta'_\ell\|_{L^2((0,T);L^2(\Omega))} + \|L\,\theta_\ell\|_{L^2((0,T);L^2(\Omega))} + k\,\|L\,\theta'_\ell\|_{L^2((0,T);L^2(\Omega))}. \tag{3.27}$$

On the other hand, the approximation properties of $\widehat{\Pi}_q, \Pi_{q-1}$ imply

$$A_2 \leqslant C\,k\,\big[\|w''_\delta\|_{L^2((0,T);L^2(\Omega))} + \|L\,w'_\delta\|_{L^2((0,T);L^2(\Omega))}\big]. \tag{3.28}$$

Using (3.4), (3.5), and (3.21), we conclude, therefore, that

$$\begin{aligned}
A_1 + A_2 + A_3 &\leqslant \beta_\ell(w_\delta) + \frac{k}{\delta^{m+1}}\tilde{\beta}_\ell\|w\|_{L^2((0,T);H^2(\Omega))}\\
&\quad + C\frac{k}{\delta}\|w\|_{H^1((0,T);L^2(\Omega))\cap L^2((0,T);H^2(\Omega))} + C\delta.
\end{aligned} \tag{3.29}$$

The proof of (3.22) is completed by suitably selecting $\delta = \delta(\ell, k)$ in order that the right-hand side of (3.29) converges to zero.

Remark 3.2 (On the abstract assumptions on $\widehat{\Pi}_q$, Π_{q-1}) Notice that the assumption (3.20) requires only that $\widehat{\Pi}_q$ is any interpolant onto piecewise polynomials of degree q which preserves continuity at the nodes, i.e., $\tilde{t}_{n0} = t_n$ and $\tilde{t}_{nq} = t_{n+1}$. For certain methods, for example, for collocation methods where the nodes include at least one endpoint of $[0,1]$ and for discontinuous Galerkin methods, one may select $\tilde{t}_{ni} = t_{ni}$, $i = 1,\dots,q$, which may be convenient from computational perspective. Assumption (3.12) requires essentially that the interpolatory quadrature induced by Π_{q-1} integrates exactly piecewise polynomials of degree q. This assumption is always satisfied by the methods considered in Section 4.

Next we shall combine the above results to show that the sequence of discrete minimizers (u_ℓ) converges in $L^2((0,T);H^1(\Omega))$ to the exact solution of our problem. We shall use the Aubin–Lions Lemma which is an analogue of the Rellich–Kondrachov theorem in the parabolic case; see, e.g., [52].

Lemma 3.3 (Aubin–Lions Lemma) *Let B_0, B, B_1 be three Banach spaces, with B_0, B_1 reflexive. Suppose that B_0 is continuously embedded into B, which is also continuously embedded into B_1, and the embedding from B_0 into B is compact. For any given p_0, p_1 with $1 < p_0, p_1 < \infty$, let*

$$W = \{v \mid v \in L^{p_0}((0,T); B_0)\ ,\ v_t \in L^{p_1}((0,T); B_1)\}. \tag{3.30}$$

Then, the embedding from W into $L^{p_0}((0,T); B)$ is compact.

We are now ready to conclude the proof of the main result of this section.

Theorem 3.1 (Convergence) *Let $\mathcal{G}$, $\mathcal{G}_\ell$ be the energy functionals defined in (3.2) and (2.14), respectively. Let u be the exact solution of (3.1) and let (u_ℓ), $u_\ell \in V_\ell$, be a sequence of minimizers of $\mathcal{G}_\ell$, i.e.,*

$$\mathcal{G}_\ell(u_\ell) = \inf_{v_\ell \in W_\ell} \mathcal{G}_\ell(v_\ell)\,. \tag{3.31}$$

Then,

$$\hat{u}_\ell \to u, \quad \text{in } L^2((0,T); H^1(\Omega)), \tag{3.32}$$

where $\hat{u}_\ell = \widehat{\Pi}_q u_\ell$.

Proof Our assumptions imply that the solution u of (3.1) satisfies $u \in L^2((0,T); H^2(\Omega) \cap H_0^1(\Omega)) \cap H^1((0,T); L^2(\Omega))$, and the elliptic regularity

$$\|u\|_{L^2((0,T);H^2(\Omega))} \leqslant C\|Lu\|_{L^2((0,T);L^2(\Omega))}$$

is valid. Consider the sequence of minimizers (u_ℓ). By their definition,

$$\mathcal{G}_\ell(u_\ell) \leqslant \mathcal{G}_\ell(v_\ell), \qquad \text{for all } v_\ell \in V_\ell\,.$$

In particular, $\mathcal{G}_\ell(u_\ell) \leqslant \mathcal{G}_\ell(\tilde{u}_\ell)$, where $\tilde{u}_\ell$ is the recovery sequence $w_{\delta,\ell}$ corresponding to $w = u$ constructed in Lemma 3.2. Since $\mathcal{G}_\ell(\tilde{u}_\ell)$ converges to $\mathcal{G}(u)$, we infer that the sequence $\mathcal{G}_\ell(u_\ell)$ is uniformly bounded. The stability of the discrete functional of Proposition 3.1 yields the uniform bound

$$\|\overline{u}_\ell\|_{L^2((0,T);H^2(\Omega))} + \|\widehat{u}_\ell\|_{L^2((0,T);H^2(\Omega))} + \|\widehat{u}'_\ell\|_{L^2((0,T);L^2(\Omega))} \leqslant C. \tag{3.33}$$

Applying the Aubin–Lions Lemma, we conclude the existence of $\tilde{u} \in L^2((0,T); H^1(\Omega))$ such that $\widehat{u}_\ell \to \tilde{u}$ in $L^2((0,T); H^1(\Omega))$ up to a subsequence not relabeled. Furthermore, the arguments in Lemma 3.1 show that $L\tilde{u} \in L^2((0,T); L^2(\Omega))$. Next we show that $\tilde{u}$ is the minimizer of $\mathcal{G}$, and hence $\tilde{u} = u$. Indeed, let $w \in H^1((0,T); L^2(\Omega)) \cap L^2((0,T); H^2(\Omega) \cap H_0^1(\Omega))$, and let (w_ℓ) be such that $w_\ell \to w$ and

$$\mathcal{G}(w) = \lim_{\ell \to \infty} \mathcal{G}_\ell(w_\ell).$$

Therefore, the lim inf inequality and the fact that u_ℓ are minimizers of the discrete problems imply that

$$\mathcal{G}(\tilde{u}) \leqslant \liminf_{\ell \to \infty} \mathcal{G}_\ell(u_\ell) \leqslant \limsup_{\ell \to \infty} \mathcal{G}_\ell(u_\ell) \leqslant \limsup_{\ell \to \infty} \mathcal{G}_\ell(w_\ell) = \mathcal{G}(w), \tag{3.34}$$

for all $w \in H^1((0,T); L^2(\Omega)) \cap L^2((0,T); H^2(\Omega) \cap H_0^1(\Omega))$. Thus, $\tilde{u}$ is the minimizer of $\mathcal{G}$, and thus $\tilde{u} = u$ and the entire sequence satisfies

$$\hat{u}_\ell \to u, \quad \text{in } L^2((0,T); H^1(\Omega)).$$

4 Discrete maximal parabolic L^2 regularity in Hilbert spaces

We consider the discretization of differential equations satisfying the maximal parabolic regularity property in Hilbert spaces by B-stable Runge–Kutta methods, the Lobatto IIIA methods, and Galerkin time-stepping methods. We establish discrete maximal parabolic L^2 regularity by the energy technique.

4.1 An abstract initial value problem

We consider an initial value problem for a linear parabolic equation,

$$\begin{cases} u'(t) + Au(t) = f(t), \quad 0 < t < T, \\ u(0) = u_0, \end{cases} \tag{4.1}$$

in a Hilbert space $(H, (\cdot,\cdot))$. We denote the induced norm by $|\cdot|$, $|v| = (v, v)^{1/2}$, $v \in H$. We assume that A is a coercive, self-adjoint, densely defined operator on H, $u_0 \in V := \mathscr{D}(A^{1/2})$, and $f \in L^2((0,T); H)$.

Taking the squares of the norms of both sides of the differential equation in (4.1), we have

$$|u'(s)|^2 + |Au(s)|^2 + 2(u'(s), Au(s)) = |f(s)|^2,$$

i.e.,

$$|u'(s)|^2 + |Au(s)|^2 + \frac{\mathrm{d}}{\mathrm{d}s}|A^{1/2}u(s)|^2 = |f(s)|^2.$$

Integration from $s = 0$ to $s = t \in (0, T]$ yields the well-known maximal L^2 regularity,

$$\begin{aligned} |A^{1/2}u(t)|^2 + \|u'\|^2_{L^2((0,t);H)} + \|Au\|^2_{L^2((0,t);H)} \\ = |A^{1/2}u_0|^2 + \|f\|^2_{L^2((0,t);H)} \quad \forall f \in L^2((0,t); H). \end{aligned} \tag{4.2}$$

In other words, for vanishing initial value u_0, the functions u' and Au are well defined and have the same regularity as their sum $u' + Au$, that is, the given forcing term f; the sum of the norms and the norm of the sum are equivalent.

We refer to the lecture notes [31] and to the review article [19] for excellent accounts of the maximal L^p-regularity theory. Coercive elliptic differential operators on $L^s(\Omega), 1 < s < \infty$, with general boundary conditions possess the maximal L^p-regularity property; see [31], [19], and references therein. For maximal L^p-regularity properties of Runge–Kutta methods, see [30] and references therein.

4.2 The numerical methods

Recall that we are using a partition of the time interval $[0,T]$ into subintervals $J_n := (t_n, t_{n+1}]$, $n = 0,\dots,N$, and $k_n = |J_n|$. Our results apply to arbitrary partitions.

For $s \in \mathbb{N}_0$, we denote by $\mathbb{P}(s)$ the space of polynomials of degree at most s with coefficients in $\mathscr{D}(A)$, the domain of the operator A, i.e., the elements g of $\mathbb{P}(s)$ are of the form

$$g(t) = \sum_{j=0}^{s} t^j w_j, \quad w_j \in \mathscr{D}(A), \quad j = 0,\dots,s.$$

With this notation, let $\mathcal{V}_k^{\mathrm{c}}(s)$ and $\mathcal{V}_k^{\mathrm{d}}(s)$ be the spaces of continuous and possibly discontinuous, respectively, piecewise elements of $\mathbb{P}(s)$,

$$\begin{aligned}\mathcal{V}_k^{\mathrm{c}}(s) &:= \{v \in C\big([0,T];\mathscr{D}(A)\big) : v|_{J_n} \in \mathbb{P}(s),\ n = 0,\dots,N-1\},\\ \mathcal{V}_k^{\mathrm{d}}(s) &:= \{v : [0,T] \to \mathscr{D}(A),\ v|_{J_n} \in \mathbb{P}(s),\ n = 0,\dots,N-1\}.\end{aligned}$$

The spaces $\mathcal{H}_k^{\mathrm{c}}(s)$ and $\mathcal{H}_k^{\mathrm{d}}(s)$ are defined analogously, with coefficients $w_j \in H$.

The numerical methods we consider here can be cast in the following abstract form: For $q \in \mathbb{N}$, and two given projection or interpolation operators $\Pi_{q-1}, \widetilde{\Pi}_{q-1} : C\big([0,T];H\big) \to \mathcal{H}_k^{\mathrm{d}}(q-1)$, seek $\widehat{U} \in \mathcal{V}_k^{\mathrm{c}}(q)$ satisfying the initial condition $\widehat{U}(0) = u_0$ and the pointwise equations

$$\widehat{U}'(t) + A\Pi_{q-1}\widehat{U}(t) = \widetilde{\Pi}_{q-1} f(t), \quad t \in (t_n, t_{n+1}], \quad n = 0,\dots,N-1. \tag{4.3}$$

Collocation methods as well as Galerkin time-stepping methods can be written in the form (4.3); see [4]. More precisely, $\widehat{U}$ is the collocation approximation and the continuous Galerkin approximation for these two classes of methods, and a suitable reconstruction of the solution for the discontinuous Galerkin method. Moreover, as we shall see, our key assumption (4.4) in Theorem 4.1 is satisfied for the Galerkin time-stepping methods as well as for some important collocation methods such as the Gauss, Radau IIA, and Lobatto IIIA methods. Furthermore, in Section 4.4.3 we show maximal regularity estimates of all algebraically stable Runge–Kutta methods.

Remark 4.1 (On the starting value) We assume that the starting value $U_0 = u_0$ belongs to $\mathscr{D}(A)$. For some methods, like the continuous Galerkin, Gauss, and Lobatto IIIA methods, this condition is needed to ensure existence of smooth approximate solutions. For methods with the *smoothing property*, in the sense that $\Pi_{q-1}\widehat{U}$ is $\mathscr{D}(A)$-valued for positive t even for $u_0 \in V = \mathscr{D}(A^{1/2})$, the milder condition $u_0 \in V$ suffices. In the latter case, the approximation $\widehat{U}$ is V-valued in the first subinterval $[0,t_1)$; it is $\mathscr{D}(A)$-valued only at the points of this subinterval where it coincides with $\Pi_{q-1}\widehat{U}$.

Theorem 4.1 (Maximal L^2 regularity for methods of the form (4.3)) *Assume that the operator Π_{q-1} in (4.3) is such that*

$$\int_{t_n}^{t_{n+1}} (\widehat{U}'(t), A\Pi_{q-1}\widehat{U}(t))\,\mathrm{d}t \geqslant \int_{t_n}^{t_{n+1}} (\widehat{U}'(t), A\widehat{U}(t))\,\mathrm{d}t = \frac{1}{2}\big(|A^{1/2}\widehat{U}(t_{n+1})|^2 - |A^{1/2}\widehat{U}(t_n)|^2\big). \tag{4.4}$$

Then, the method satisfies the following discrete analogue of the continuous maximal L^2 regularity property (4.2)

$$|A^{1/2}\widehat{U}(t_m)|^2 + \|\widehat{U}'\|^2_{L^2((0,t_m);H)} + \|A\Pi_{q-1}\widehat{U}\|^2_{L^2((0,t_m);H)} \leqslant |A^{1/2}\widehat{U}(0)|^2 + \|\widetilde{\Pi}_{q-1}f\|^2_{L^2((0,t_m);H)} \tag{4.5}$$

for $m = 1, \dots, N$.

Proof Taking the squares of the norms of both sides of the pointwise form (4.3) of the abstract numerical method, we infer that

$$|\widehat{U}'(t)|^2 + |A\Pi_{q-1}\widehat{U}(t)|^2 + 2(\widehat{U}'(t), A\Pi_{q-1}\widehat{U}(t)) = |\widetilde{\Pi}_{q-1}f(t)|^2, \quad t \in (t_n, t_{n+1}].$$

Integration over $J_n = (t_n, t_{n+1}]$ yields

$$\int_{t_n}^{t_{n+1}} |\widehat{U}'(t)|^2\,\mathrm{d}t + \int_{t_n}^{t_{n+1}} |A\Pi_{q-1}\widehat{U}(t)|^2\,\mathrm{d}t + 2\int_{t_n}^{t_{n+1}} (\widehat{U}'(t), A\Pi_{q-1}\widehat{U}(t))\,\mathrm{d}t = \int_{t_n}^{t_{n+1}} |\widetilde{\Pi}_{q-1}f(t)|^2\,\mathrm{d}t. \tag{4.6}$$

Now, utilizing our assumption (4.4) in (4.6), we can estimate the last term on the left-hand side from below and obtain

$$|A^{1/2}\widehat{U}(t_{n+1})|^2 + \int_{t_n}^{t_{n+1}} |\widehat{U}'(t)|^2\,\mathrm{d}t + \int_{t_n}^{t_{n+1}} |A\Pi_{q-1}\widehat{U}(t)|^2\,\mathrm{d}t \leqslant |A^{1/2}\widehat{U}(t_n)|^2 + \int_{t_n}^{t_{n+1}} |\widetilde{\Pi}_{q-1}f(t)|^2\,\mathrm{d}t. \tag{4.7}$$

Summation over n from $n = 0$ to $n = m - 1 \leqslant N - 1$, yields the asserted maximal regularity estimate (4.5).

4.3 Galerkin time-stepping methods

4.3.1 Continuous Galerkin methods

For $q \in \mathbb{N}$, with starting value $U(0) = u_0$, we consider the discretization of the initial value problem (4.1) by the *continuous Galerkin method* cG(q), i.e., we seek $\widehat{U} \in \mathcal{V}_k^{\mathrm{c}}(q)$ such that

$$\int_{J_n} \big((\widehat{U}', v) + (A\widehat{U}, v)\big)\,\mathrm{d}t = \int_{J_n} (f, v)\,\mathrm{d}t \quad \forall v \in \mathbb{P}(q-1) \tag{4.8}$$

for $n = 0, \dots, N-1$. Denoting by P_{q-1} the piecewise L^2-projection onto $\mathcal{H}^{\mathrm{d}}_k(q-1)$ and using the fact that $\widehat{U}' \in \mathcal{V}^{\mathrm{d}}_k(q-1)$, we see that the *pointwise form* of (4.8) is

$$\widehat{U}' + AP_{q-1}\widehat{U} = P_{q-1}f, \tag{4.9}$$

which is (4.3) with $\Pi_{q-1} := \widetilde{\Pi}_{q-1} := P_{q-1}$.

In this case, since $\widehat{U}' \in \mathcal{V}^{\mathrm{d}}_k(q-1)$, we have

$$\int_{t_n}^{t_{n+1}} (\widehat{U}'(t), A\widehat{U}(t) - AP_{q-1}\widehat{U}(t))\,\mathrm{d}t = 0$$

and see that the key assumption (4.4) holds true as an equality.

It will be useful to observe the following relation

$$\int_{t_n}^{t_{n+1}} (\varphi, I_{G,q-1}W(t))\,\mathrm{d}t = \int_{t_n}^{t_{n+1}} (\varphi, W(t))\,\mathrm{d}t \quad \forall \varphi \in \mathbb{P}(q-1)\,, \tag{4.10}$$

where $W \in \mathbb{P}(q)$ and $I_{G,q-1}v \in \mathbb{P}(q-1)$ denotes the interpolant of v at the q Gauss points of J_n; indeed, the integrand $(\varphi, W - I_{G,q-1}W) \in \mathbb{P}_{2q-1}$ is integrated exactly by the Gauss quadrature formula with q nodes and it vanishes at these nodes. Therefore,

$$P_{q-1}|_{\mathbb{P}(q)} = I_{G,q-1}.$$

Therefore, as an immediate consequence of Theorem 4.1, we have the following maximal L^2 regularity of cG methods:

Proposition 4.1 (Maximal L^2 regularity of cG methods) *The cG methods satisfy the following analogue of the continuous maximal L^2 regularity property* (4.2)

$$\begin{aligned} &|A^{1/2}\widehat{U}(t_m)|^2 + \|\widehat{U}'\|^2_{L^2((0,t_m);H)} + \|AP_{q-1}\widehat{U}\|^2_{L^2((0,t_m);H)} \\ &= |A^{1/2}\widehat{U}(t_m)|^2 + \|\widehat{U}'\|^2_{L^2((0,t_m);H)} + \|AI_{G,q-1}\widehat{U}\|^2_{L^2((0,t_m);H)} \\ &= |A^{1/2}\widehat{U}(0)|^2 + \|P_{q-1}f\|^2_{L^2((0,t_m);H)} \end{aligned} \tag{4.11}$$

for $m = 1, \dots, N$.

Since, obviously,

$$\begin{aligned} &\int_{t_n}^{t_{n+1}} |P_{q-1}f(t)|^2\,\mathrm{d}t \leqslant \int_{t_n}^{t_{n+1}} |f(t)|^2\,\mathrm{d}t \\ &\implies \|P_{q-1}f\|^2_{L^2((0,t_m);H)} \leqslant \|f\|^2_{L^2((0,t_m);H)}, \end{aligned} \tag{4.12}$$

(4.11) yields also the estimate

$$\begin{aligned} &|A^{1/2}\widehat{U}(t_m)|^2 + \|\widehat{U}'\|^2_{L^2((0,t_m);H)} + \|AP_{q-1}\widehat{U}\|^2_{L^2((0,t_m);H)} \\ &\qquad \leqslant |A^{1/2}\widehat{U}(0)|^2 + \|f\|^2_{L^2((0,t_m);H)} \end{aligned} \tag{4.13}$$

for $m = 1, \dots, N$.

4.3.2 Discontinuous Galerkin methods

For $q \in \mathbb{N}$, with starting value $U(0) = u_0$, we consider the discretization of the initial value problem (4.1) by the *discontinuous Galerkin method* $\mathrm{dG}(q-1)$, i.e., we seek $U \in \mathcal{V}_k^{\mathrm{d}}(q-1)$ such that

$$\int_{J_n} \big((U',v)+(AU,v)\big)\,\mathrm{d}t+(U_n^+-U_n,v_n^+) = \int_{J_n}(f,v)\,\mathrm{d}t \quad \forall v \in \mathbb{P}(q-1) \tag{4.14}$$

for $n = 0,\dots,N-1$. As usual, we use the notation $v_n := v(t_n)$, $v_n^+ := \lim_{s\searrow 0} v(t_n+s)$.

Following [36], we define the *reconstruction* $\widehat{U}$ of the dG approximation U, the analogue of the collocation approximation, by extended interpolation at the Radau nodes $t_{ni} = t_n + c_i k_n, 0 < c_1 < \cdots < c_q = 1$,

$$\widehat{U}(t_{ni}) = U(t_{ni}), \quad i = 0,\dots,q \quad (U(t_{n0}) = U_n).$$

The reconstruction satisfies the relations

$$\begin{aligned} &\widehat{U}_n^+ = U_n, \\ &\int_{J_n}(\widehat{U}',v)\,\mathrm{d}t = \int_{J_n}(U',v)\,\mathrm{d}t + (U_n^+ - U_n, v_n^+) \quad \forall v \in \mathbb{P}(q-1). \end{aligned} \tag{4.15}$$

Consequently, we can reformulate the discontinuous Galerkin method (4.14) as

$$\int_{J_n}\big((\widehat{U}',v)+(AU,v)\big)\,\mathrm{d}t = \int_{J_n}(f,v)\,\mathrm{d}t \quad \forall v \in \mathbb{P}(q-1). \tag{4.16}$$

Denoting again by P_{q-1} the piecewise L^2-projection onto $\mathcal{H}_k^{\mathrm{d}}(q-1)$, we see that the *pointwise form* of (4.16) is

$$\widehat{U}' + AU = P_{q-1}f, \tag{4.17}$$

i.e.,

$$\widehat{U}' + AI_{q-1}\widehat{U} = P_{q-1}f, \tag{4.18}$$

which is (4.3) with $\Pi_{q-1} := I_{q-1}$, the interpolation operator at the Radau nodes, and $\widetilde{\Pi}_{q-1} := P_{q-1}$.

Let us now see that our key assumption (4.4) is satisfied also in this case, i.e., that

$$\int_{t_n}^{t_{n+1}}\big(\widehat{U}'(t), A(\widehat{U}(t) - I_{q-1}\widehat{U}(t))\big)\,\mathrm{d}t \leqslant 0. \tag{4.19}$$

It is advantageous to reformulate (4.19) in the form

$$\begin{aligned} &\int_{t_n}^{t_{n+1}}\big((\widehat{U} - I_{q-1}\widehat{U})'(t), A(\widehat{U}(t) - I_{q-1}\widehat{U}(t))\big)\,\mathrm{d}t \\ &+ \int_{t_n}^{t_{n+1}}\big((I_{q-1}\widehat{U})'(t), A(\widehat{U}(t) - I_{q-1}\widehat{U}(t))\big)\,\mathrm{d}t \leqslant 0. \end{aligned} \tag{4.20}$$

Now, the integrand $\tilde{\pi} := \big((I_{q-1}\widehat{U})'(\cdot), A(\widehat{U}(\cdot) - I_{q-1}\widehat{U}(\cdot))\big)$ in the second integral in (4.20) is a polynomial of degree at most $2q-2$; therefore, $\tilde{\pi}$ is integrated exactly by the Radau quadrature formula with q nodes. Furthermore, $\tilde{\pi}$ vanishes at the quadrature nodes $t_{n1}, \dots, t_{nq}$. Thus, the second integral vanishes, and (4.19) can be written in the form

$$\int_{t_n}^{t_{n+1}} \big(\widehat{U}'(t) - (I_{q-1}\widehat{U})'(t), A(\widehat{U}(t) - I_{q-1}\widehat{U}(t))\big)\,\mathrm{d}t \leqslant 0,$$

i.e.,

$$\frac{1}{2}\int_{t_n}^{t_{n+1}} \frac{\mathrm{d}}{\mathrm{d}t}|A^{1/2}(\widehat{U}(t) - I_{q-1}\widehat{U}(t))|^2\,\mathrm{d}t \leqslant 0,$$

that is, since $t_{nq} = t_{n+1}$,

$$-\frac{1}{2}|A^{1/2}(\widehat{U}(t_n) - (I_{q-1}\widehat{U})(t_{n+}))|^2 \leqslant 0,$$

which is obviously valid. Therefore, (4.19) is valid.

In view of (4.19), as an immediate consequence of Theorem 4.1, we have the following maximal L^2 regularity of dG methods:

Proposition 4.2 (Maximal L^2 regularity of dG methods) *The dG methods satisfy the following analogue of the continuous maximal L^2 regularity property* (4.2)

$$\begin{aligned}|A^{1/2}\widehat{U}(t_m)|^2 + \|\widehat{U}'\|^2_{L^2((0,t_m);H)} + \|AU\|^2_{L^2((0,t_m);H)}\\ \leqslant |A^{1/2}\widehat{U}(0)|^2 + \|P_{q-1}f\|^2_{L^2((0,t_m);H)}\end{aligned} \tag{4.21}$$

for $m = 1, \dots, N$.

In view of (4.12), (4.17) yields also the estimate

$$\begin{aligned}|A^{1/2}\widehat{U}(t_m)|^2 + \|\widehat{U}'\|^2_{L^2((0,t_m);H)} + \|AU\|^2_{L^2((0,t_m);H)}\\ \leqslant |A^{1/2}\widehat{U}(0)|^2 + \|f\|^2_{L^2((0,t_m);H)}\end{aligned} \tag{4.22}$$

for $m = 1, \dots, N$.

4.4 Collocation Runge–Kutta methods

For $q \in \mathbb{N}$, let $0 \leqslant c_1 < \cdots < c_q \leqslant 1$ denote the collocation nodes. The collocation approximation $\widehat{U} \in \mathcal{V}_k^{\mathrm{c}}(q)$ satisfies the initial condition $\widehat{U}(0) = u_0$ as well as the collocation conditions

$$\widehat{U}'(t_{ni}) + A\widehat{U}(t_{ni}) = f(t_{ni}), \quad i = 1, \dots, q, \quad n = 0, \dots, N-1. \tag{4.23}$$

Here, we assumed that $f(t) \in H$ for $t \in [0, T]$. Thus, [3] and [4], if we let $I_{q-1} : C\big([0,T]; H\big) \to \mathcal{H}_k^{\mathrm{d}}(q-1)$ denote the interpolation operator at the

collocation nodes $t_{ni}, i = 1, \dots, q, n = 0, \dots, N-1$, and use the fact that $\widehat{U}' \in \mathcal{V}_k^{\mathrm{d}}(q-1)$, we can write (4.23) in *pointwise form* as

$$\widehat{U}'(t) + AI_{q-1}\widehat{U}(t) = I_{q-1}f(t), \quad t \in (t_n, t_{n+1}], \quad n = 0, \dots, N-1, \tag{4.24}$$

which is (4.3) with $\Pi_{q-1} := \widetilde{\Pi}_{q-1} := I_{q-1}$. The interpolants $U := I_{q-1}\widehat{U}$ and $I_{q-1}f$ are elements of $\mathcal{V}_k^{\mathrm{d}}(q-1)$ and $\mathcal{H}_k^{\mathrm{d}}(q-1)$, respectively, and thus, in general, for positive c_1, discontinuous at the nodes $t_0, \dots, t_{N-1}$.

The corresponding q-stage Runge–Kutta method is specified by the coefficients

$$a_{ij} = \int_0^{c_i} \ell_j(\tau)\,\mathrm{d}\tau, \quad b_i = \int_0^1 \ell_i(\tau)\,\mathrm{d}\tau, \quad i, j = 1, \dots, q; \tag{4.25}$$

here, $\ell_1, \dots, \ell_q \in \mathbb{P}_{q-1}$ are the Lagrange polynomials for the collocation nodes $c_1, \dots, c_q$, $\ell_i(c_j) = \delta_{ij}, i, j = 1, \dots, q$. In other words, the *stage order* of the Runge–Kutta method is q.

With starting value $U_0 = u_0$, we now consider the discretization of the initial value problem (4.1) by the q-stage Runge–Kutta method (4.25): we recursively define approximations $U_\ell \in \mathscr{D}(A)$ to the nodal values $u(t_\ell)$, as well as internal approximations $U_{\ell i} \in \mathscr{D}(A)$ to the intermediate values $u(t_{\ell i})$, by

$$\begin{cases} U_{ni} = U_n - k_n \sum_{j=1}^{q} a_{ij}\big(AU_{nj} - f(t_{nj})\big), \quad i = 1, \dots, q, \\ U_{n+1} = U_n - k_n \sum_{i=1}^{q} b_i\big(AU_{ni} - f(t_{ni})\big), \end{cases} \tag{4.26}$$

$n = 0, \dots, N-1$. Here, we assumed that $f(t) \in H$ for $t \in [0, T]$.

It is well known that the collocation and Runge–Kutta methods (4.23) and (4.26), respectively, are equivalent in the sense that they yield the same approximations at the nodes and at the intermediate nodes, i.e.,

$$\begin{aligned} &\widehat{U}(t_n) = U_n, \quad && n = 1, \dots, N, \\ &\widehat{U}(t_{ni}) = U_{ni}, \quad && i = 1, \dots, q, \ \ n = 0, \dots, N-1. \end{aligned} \tag{4.27}$$

4.4.1 Maximal regularity of Gauss and Radau IIA methods

We treat this case separately for various reasons: (i) These two families of Runge–Kutta methods are particularly interesting and popular for parabolic equations. (ii) The methods satisfy our key assumption (4.4) and, consequently, discrete analogues of the continuous maximal L^2 regularity property (4.2), with inequality in the place of the equality for the Radau IIA methods. (iii) The proofs are short and elegant, immediate consequences of the abstract result in Theorem 4.1.

We have already seen that assumption (4.4) is satisfied for the Radau IIA methods; see (4.18) and recall that I_{q-1} there is the interpolation operator at the Radau nodes $t_{n1}, \dots, t_{nq}$.

Now, we will see that the Gauss method satisfies (4.19) as an equality, with I_{q-1} now, of course, the interpolation operator at the Gauss nodes $t_{n1}, \dots, t_{nq}$. Indeed, the integrand $\pi := \big(\widehat{U}'(\cdot), A(\widehat{U}(\cdot) - I_{q-1}\widehat{U}(\cdot))\big)$ in (4.19) is a polynomial of degree at most $2q-1$; therefore, π is integrated exactly by the Gauss quadrature formula with q nodes. Furthermore, π vanishes at the quadrature nodes $t_{n1}, \dots, t_{nq}$. Thus, (4.19) holds as an equality in this case.

In view of (4.19), as an immediate consequence of Theorem 4.1, we have the following maximal L^2 regularity property for Gauss and Radau IIA methods:

Proposition 4.3 (Maximal L^2 regularity of Gauss and Radau IIA methods) *The Gauss and Radau IIA methods satisfy the exact discrete analogues of the continuous maximal L^2 regularity property (4.2), namely,*

$$\begin{aligned} |A^{1/2}\widehat{U}(t_m)|^2 + \|\widehat{U}'\|^2_{L^2((0,t_m);H)} + \|AI_{q-1}\widehat{U}\|^2_{L^2((0,t_m);H)} \\ \leqslant |A^{1/2}\widehat{U}(0)|^2 + \|I_{q-1}f\|^2_{L^2((0,t_m);H)}, \end{aligned} \tag{4.28}$$

for $m = 1, \dots, N$, with equality for the Gauss methods.

Let us now give an alternative form of (4.28).

Proposition 4.4 (Alternative form of the maximal L^2 regularity of Gauss and Radau IIA methods) *Let $0 < c_1, \dots, c_q \leqslant 1$ and $b_1, \dots, b_q$ be the nodes and the weights of the Gauss and Radau quadrature formulas in the interval $[0,1]$, respectively. Then, the Gauss and Radau IIA methods satisfy the maximal L^2 regularity property*

$$\begin{aligned} |A^{1/2}U_m|^2 + \sum_{n=0}^{m-1} k_n \sum_{i=1}^{q} b_i |\widehat{U}'(t_{ni})|^2 + \sum_{n=0}^{m-1} k_n \sum_{i=1}^{q} b_i |AU_{ni}|^2 \\ \leqslant |A^{1/2}U_0|^2 + \sum_{n=0}^{m-1} k_n \sum_{i=1}^{q} b_i |f(t_{ni})|^2 \end{aligned} \tag{4.29}$$

for $m = 1, \dots, N$, with equality for the Gauss methods. Here, in the case of the Radau IIA methods, $\widehat{U}'(t_{nq})$ stands for the left-hand derivative at t_{n+1}, $\lim_{t \nearrow t_{n+1}} \widehat{U}'(t)$.

Proof Obviously, $|\widehat{U}'|^2$, $|AI_{q-1}\widehat{U}|^2$, and $|I_{q-1}f|^2$ are integrated exactly by both the Gauss and Radau quadrature formulas in each subinterval $[t_n, t_{n+1}]$ as polynomials of degree at most $2q-2$. Consequently, for instance,

$$\int_{t_n}^{t_{n+1}} |\widehat{U}'(t)|^2 \, \mathrm{d}t = k_n \sum_{i=1}^{q} b_i |\widehat{U}'(t_{ni})|^2,$$

and (4.28) can be equivalently written in the form (4.29).

4.4.2 Maximal regularity of Lobatto IIIA methods

Here, we focus on the Lobatto IIIA methods, which are A-stable but are not B-stable. So, for $q \in \mathbb{N}$, let $0 = c_1 < \cdots < c_q = 1$ denote the Lobatto nodes; then, the collocation approximation $\widehat{U} \in \mathcal{V}_k^{\mathrm{c}}(q)$ satisfies the initial condition $\widehat{U}(0) = u_0$ as well as the collocation conditions

$$\widehat{U}'(t_{ni}) + A\widehat{U}(t_{ni}) = f(t_{ni}), \quad i = 1, \dots, q, \quad n = 0, \dots, N-1. \tag{4.30}$$

We assumed that $f(t) \in H$ for $t \in [0, T]$. In this case, the pointwise form of the method is again

$$\widehat{U}'(t) + AI_{q-1}\widehat{U}(t) = I_{q-1}f(t), \quad t \in (t_n, t_{n+1}], \quad n = 0, \dots, N-1; \tag{4.31}$$

compare to (4.24). Notice, however, the important fact that the interpolants $\widetilde{U} := I_{q-1}\widehat{U}$ and $I_{q-1}f$ are now elements of $\mathcal{V}_k^{\mathrm{c}}(q-1)$ and $\mathcal{H}_k^{\mathrm{c}}(q-1)$, respectively, since $c_0 = 0$ and $c_q = 1$, and *thus are continuous functions at the nodes* $t_0, \dots, t_{N-1}$.

Now, we claim that the interpolant $\widetilde{U} = I_{q-1}\widehat{U} \in \mathcal{V}_k^{\mathrm{c}}(q-1)$ of the Lobatto collocation approximation $\widehat{U}$ is the solution of a *modified* continuous Galerkin (cG) method in $\mathcal{V}_k^{\mathrm{c}}(q-1)$, namely, $\widetilde{U} \in \mathcal{V}_k^{\mathrm{c}}(q-1)$ is such that

$$\int_{t_n}^{t_{n+1}} \big((\widetilde{U}', v) + (A\widetilde{U}, v)\big)\,\mathrm{d}t = \int_{J_n} (I_{q-1}f, v)\,\mathrm{d}t \quad \forall v \in \mathbb{P}(q-2) \tag{4.32}$$

for $n = 0, \dots, N-1$, with the modification consisting in the fact that the forcing term f on the right-hand side has been replaced by its interpolant $I_{q-1}f$. Compare to (4.8) and notice that (4.32) is a modification of the cG$(q-1)$ rather than the cG(q) method.

Now, (4.31) implies

$$\int_{t_n}^{t_{n+1}} \big((\widehat{U}', v) + (A\widetilde{U}, v)\big)\,\mathrm{d}t = \int_{t_n}^{t_{n+1}} (I_{q-1}f, v)\,\mathrm{d}t \quad \forall v \in \mathbb{P}(q-2) \tag{4.33}$$

for $n = 0, \dots, N-1$. In view of the fact that $\widetilde{U} = I_{q-1}\widehat{U}$, (4.32) follows immediately from (4.31) provided

$$\int_{t_n}^{t_{n+1}} (\widehat{U}' - (I_{q-1}\widehat{U})', v)\,\mathrm{d}t = 0 \quad \forall v \in \mathbb{P}(q-2). \tag{4.34}$$

Since $(I_{q-1}\widehat{U})(t_m) = \widehat{U}(t_m)$, integrating by parts, we can rewrite (4.34) as

$$\int_{t_n}^{t_{n+1}} (\widehat{U} - I_{q-1}\widehat{U}, v')\,\mathrm{d}t = 0 \quad \forall v \in \mathbb{P}(q-2). \tag{4.35}$$

Now, the integrand $\pi := \big(\widehat{U}(\cdot) - I_{q-1}\widehat{U}(\cdot), v'(\cdot)\big)$ in (4.35) is a polynomial of degree at most $2q-3$; therefore, π is integrated exactly by the Lobatto quadrature formula with q nodes. Furthermore, π vanishes at the quadrature nodes $t_{n1}, \dots, t_{nq}$. Thus, (4.35), and hence also (4.34), is indeed valid.

It is straightforward now to apply the maximal regularity estimate for the continuous Galerkin method to conclude:

Proposition 4.5 (Maximal L^2 regularity of Lobatto IIIA methods) *Let $I_{G,q-2}v \in \mathbb{P}(q-2)$ denote the interpolant of v at the $q-1$ Gauss points of J_n. The Lobatto IIIA methods satisfy the following analogue of the continuous maximal L^2 regularity property (4.2)*

$$\begin{aligned} &|A^{1/2}U_m|^2 + \|\widetilde{U}'\|^2_{L^2((0,t_m);H)} + \|AI_{G,q-2}\widetilde{U}\|^2_{L^2((0,t_m);H)} \\ &\qquad = |A^{1/2}U_0|^2 + \|P_{q-2}I_{q-1}f\|^2_{L^2((0,t_m);H)} \end{aligned} \tag{4.36}$$

and

$$\begin{aligned} &|A^{1/2}U_m|^2 + \|\widetilde{U}'\|^2_{L^2((0,t_m);H)} + \|AI_{G,q-2}\widetilde{U}\|^2_{L^2((0,t_m);H)} \\ &\qquad \leqslant |A^{1/2}U_0|^2 + \|I_{q-1}f\|^2_{L^2((0,t_m);H)} \end{aligned} \tag{4.37}$$

for $m = 1, \dots, N$.

Remark 4.2 (The Trapezoidal Method) It is interesting to note that for the trapezoidal method, one is able to prove directly the maximal regularity property,

$$\begin{aligned} |A^{1/2}U_m|^2 &+ \sum_{n=0}^{m-1} k_n \Big| \frac{U_{n+1}-U_n}{k_n} \Big|^2 + \sum_{n=0}^{m-1} k_n \Big| \frac{AU_{n+1}+AU_n}{2} \Big|^2 \\ &= |A^{1/2}U_0|^2 + \sum_{n=0}^{m-1} k_n \Big| \frac{f(t_{n+1})+f(t_n)}{2} \Big|^2, \end{aligned} \tag{4.38}$$

which is identical to (4.36) for $q = 2$. Hence, (4.36) is a natural but nonobvious generalization of (4.38).

Remark 4.3 (Alternative version of (4.38)) Maximal regularity estimates of the form

$$\sum_{n=0}^{m-1} k \Big| \frac{U_{n+1}-U_n}{k} \Big|^2 + \sum_{n=1}^{m} k|AU_n|^2 \leqslant C \sum_{n=0}^{m} k|f(t_n)|^2 \tag{4.39}$$

for the trapezoidal method for constant time steps, and for $U_0 = 0$, are established in [30, Theorem 3.2], actually for any $p \in (1, \infty)$ and for general UMD Banach spaces. An advantage of (4.38) is that it holds as an equality and it is valid for arbitrary partitions. High order Lobatto IIIA methods are not included in the analysis in [30, Theorem 3.2].

Remark 4.4 (Equivalence between $\widehat{U}$ and $\widetilde{U}$) If the Lobatto collocation approximation $\widehat{U}$ is available in a subinterval $\bar{J}_n = [t_n, t_{n+1}]$, then $\widetilde{U} \in \mathbb{P}(q-1)$ is obviously the interpolant of $\widehat{U}$ at the Lobatto nodes,

$$\widetilde{U}(t_{ni}) = \widehat{U}(t_{ni}), \quad i = 1, \dots, q. \tag{4.40}$$

Conversely, it $\widetilde{U}$ is available in $\bar{J}_n$, then the Lobatto collocation approximation $\widehat{U} \in \mathbb{P}(q)$ is uniquely determined by the interpolation conditions

$$\widehat{U}(t_{ni}) = \widetilde{U}(t_{ni}), \quad i = 1, \dots, q, \quad \widehat{U}'(t_n) = -A\widetilde{U}(t_n) + f(t_n). \tag{4.41}$$

4.4.3 Maximal regularity of algebraically stable Runge–Kutta methods

Our main assumption on the Runge–Kutta method is that it is B-stable. Since the collocation nodes $c_1, \dots, c_q$ are pairwise distinct, it is well known that the B-stability is equivalent to the *algebraic stability* of the method; in other words, the weights $b_1, \dots, b_q$ are nonnegative and the $q \times q$ symmetric matrix M with entries $m_{ij} := b_i a_{ij} + b_j a_{ji} - b_i b_j, i, j = 1, \dots, q$, is positive semidefinite,

$$b_i \geqslant 0, \quad i = 1, \dots, q, \quad \text{and} \quad M \in \mathbb{R}^{q,q} \ \text{ is positive semidefinite.} \tag{4.42}$$

Notice that, in the case of positive c_1, the coefficient matrix $\mathcal{A} := (a_{ij})_{i,j=1,\dots,q} \in \mathbb{R}^{q,q}$ of the Runge–Kutta method is invertible since the collocation nodes $c_1, \dots, c_q$ are pairwise distinct and positive.

In the following calculations we closely follow the proof that algebraically stable methods are B-stable. With $\varphi_j := -k_n\big(AU_{nj} - f(t_{nj})\big) = -k_n\widehat{U}'(t_{nj}) \in \mathscr{D}(A)$ (see (4.23) and (4.27)), we apply $A^{1/2}$ to (4.26) and write it in the form

$$\begin{cases} A^{1/2}U_{ni} = A^{1/2}U_n + A^{1/2}\displaystyle\sum_{j=1}^{q} a_{ij}\varphi_j, \quad i = 1, \dots, q, \\[2ex] A^{1/2}U_{n+1} = A^{1/2}U_n + A^{1/2}\displaystyle\sum_{i=1}^{q} b_i\varphi_i. \end{cases} \tag{4.43}$$

We take the squares of the norms of both sides of the second relation of (4.43), use the notation $\langle\!\langle v, w\rangle\!\rangle := (A^{1/2}v, A^{1/2}w)$ for the A-induced inner product, and obtain

$$|A^{1/2}U_{n+1}|^2 = |A^{1/2}U_n|^2 + 2\sum_{i=1}^{q} b_i\langle\!\langle\varphi_i, U_n\rangle\!\rangle + \sum_{i,j=1}^{q} b_i b_j\langle\!\langle\varphi_i, \varphi_j\rangle\!\rangle. \tag{4.44}$$

Using here the first relations of (4.43) we get

$$\sum_{i=1}^{q} b_i\langle\!\langle\varphi_i, U_n\rangle\!\rangle = \sum_{i=1}^{q} b_i\langle\!\langle\varphi_i, U_{ni}\rangle\!\rangle - \sum_{i,j=1}^{q} b_i a_{ij}\langle\!\langle\varphi_i, \varphi_j\rangle\!\rangle,$$

and (4.44) leads to

$$|A^{1/2}U_{n+1}|^2 = |A^{1/2}U_n|^2 - \sum_{i,j=1}^{q} m_{ij}\langle\!\langle\varphi_i, \varphi_j\rangle\!\rangle + 2\sum_{i=1}^{q} b_i(\varphi_i, AU_{ni}),$$

and, in view of the positive semidefiniteness of the matrix M, to

$$|A^{1/2}U_{n+1}|^2 \leqslant |A^{1/2}U_n|^2 + 2\sum_{i=1}^{q} b_i(\varphi_i, AU_{ni}). \tag{4.45}$$

Replacing φ_i by $-k_n\big(AU_{ni} - f(t_{ni})\big)$ in the second term on the right-hand side, we obtain

$$\begin{aligned}(\varphi_i, AU_{ni}) &= -k_n(AU_{ni}, AU_{ni}) + k_n(f(t_{ni}), AU_{ni})\\ &= -k_n|AU_{ni}|^2 + k(f(t_{ni}), AU_{ni});\end{aligned}$$

thus, (4.45) yields

$$|A^{1/2}U_{n+1}|^2 + 2k_n\sum_{i=1}^{q} b_i|AU_{ni}|^2 \leqslant |A^{1/2}U_n|^2 + 2k_n\sum_{i=1}^{q} b_i(f(t_{ni}), AU_{ni}). \tag{4.46}$$

Using here the binomial identity

$$\begin{aligned}2(f(t_{ni}), AU_{ni}) &= -|AU_{ni} - f(t_{ni})|^2 + |AU_{ni}|^2 + |f(t_{ni})|^2\\ &= -|\widehat{U}'(t_{ni})|^2 + |AU_{ni}|^2 + |f(t_{ni})|^2,\end{aligned}$$

we infer that

$$\begin{aligned}&|A^{1/2}U_{n+1}|^2 + k_n\sum_{i=1}^{q} b_i|\widehat{U}'(t_{ni})|^2 + k_n\sum_{i=1}^{q} b_i|AU_{ni}|^2\\ &\qquad\leqslant |A^{1/2}U_n|^2 + k_n\sum_{i=1}^{q} b_i|f(t_{ni})|^2.\end{aligned} \tag{4.47}$$

Summing here over n from $n = 0$ to $n = m-1 \leqslant N-1$, we obtain the maximal regularity estimate

$$\begin{aligned}&|A^{1/2}U_m|^2 + \sum_{n=0}^{m-1} k_n\sum_{i=1}^{q} b_i|\widehat{U}'(t_{ni})|^2 + \sum_{n=0}^{m-1} k_n\sum_{i=1}^{q} b_i|AU_{ni}|^2\\ &\qquad\leqslant |A^{1/2}U_0|^2 + \sum_{n=0}^{m-1} k_n\sum_{i=1}^{q} b_i|f(t_{ni})|^2,\end{aligned} \tag{4.48}$$

$m = 1, \dots, N$, a discrete analogue of (4.2). Notice that (4.48) reduces to (4.29) for the Gauss and Radau IIA methods.

5 General evolution problems and numerical results

5.1 Problem Setup

In this section we present numerical results for the Runge–Kutta PINNs for both linear parabolic and wave equations. We would like to demonstrate that the resulting methods work as expected and in addition preserve the qualitative behavior of Runge–Kutta methods. We begin with the following general setup of the problem. Let $u : \Omega \times (0, T] \to \mathbb{R}^M$, where $T > 0$ and $u = u(x, t)$

is a vector-valued function with M components. Let A be a differential operator acting on u which involves spatial derivatives. Our general initial value problem can be written as follows:

$$u_t + Au = f(x,t), \quad (x,t) \in \Omega \times [0,T], \tag{5.1}$$

$$u(x,0) = u_0, \quad x \in \Omega, \tag{5.2}$$

with additional boundary conditions for $t \in [0,T]$. In the numerical experiments below the boundary conditions are either Neumann (for the heat equation) or Dirichlet (for the wave equation). The formulation of the methods can be directly extended to nonlinear evolution equations with the obvious modifications in the loss functionals; see [3].

5.2 Collocation Runge–Kutta Formulation

Let the collocation points on $[t_n, t_{n+1}]$ be defined by $t_{ni} = t_n + c_i k_n$, $i = 1, \dots, q$, where $0 \leqslant c_1 < c_2 < \cdots < c_q \leqslant 1$, and $k_n = t_{n+1} - t_n$ is the width of each interval.

Furthermore, we let $0 = \tilde{c}_0 < \tilde{c}_1 < \cdots < \tilde{c}_q = 1$ be auxiliary points as introduced in Section 2.4.2, and

$$\hat{u}(x,t) = \hat{I}_q u(x,t) = \sum_{i=0}^{q} \tilde{\ell}_{ni}(t) u(x, \tilde{t}_{ni}) = \sum_{i=0}^{q} \tilde{\ell}_i \left(\frac{t - t_n}{k_n} \right) u(x, \tilde{t}_{ni}), \tag{5.3}$$

where $\tilde{t}_{ni} = t_n + \tilde{c}_i k_n$. As it will become clear in Section 5.4, in the case of Radau IIA and Lobatto IIIA methods, the points $0 = \tilde{c}_0 < \tilde{c}_1 < \cdots < \tilde{c}_q = 1$ include all the collocation points $c_1, \dots, c_q$.

Furthermore we need to interpolate at the collocation points the function $\hat{u}(x,t)$, i.e.,

$$LI_{q-1}\hat{u}(x,t) = \sum_{j=1}^{q} \ell_j \left(\frac{t - t_n}{k_n} \right) \sum_{i=0}^{q} \tilde{\ell}_i \left(\frac{t_{nj} - t_n}{k_n} \right) Lu(x, \tilde{t}_{ni}). \tag{5.4}$$

Consider a fixed interval $[t_n, t_{n+1}]$. Recall that in the loss, one has to evaluate integrals of

$$\hat{u}_t(x,t) + LI_{q-1}\hat{u}(x,t) =: \zeta(x,t), \qquad t \in [t_n, t_{n+1}], \quad x \in \Omega. \tag{5.5}$$

At the colocation points $\{t_{nj}\}_{j=1}^{q}$ it is straightforward to express the time derivative of $\hat{u}$ and the interpolant $I_{q-1}L\hat{u}$ as follows:

(5.6)

$$\hat{u}_t(x, t_{nj}) = k_n^{-1} \sum_{i=0}^{q} \tilde{\ell}_i'(c_j) u(x, \tilde{t}_{ni}), \quad LI_{q-1}\hat{u}(x, t_{nj}) = \sum_{i=0}^{q} \tilde{\ell}_i(c_j) Lu(x, \tilde{t}_{ni}).$$

Within the subinterval $[t_n, t_{n+1}]$, we have

$$\begin{aligned}\zeta(x,t_{nj}) =& \hat{u}_t(x,t_{nj}) + LI_{q-1}\hat{u}(x,t_{nj}) \\ =& \sum_{i=0}^{q} \left(k_n^{-1}\tilde{\ell}_i'(c_j)u(x,\tilde{t}_{nj}) - \tilde{\ell}_i(c_j)Lu(x,\tilde{t}_{nj})\right), \quad x \in \Omega,\end{aligned} \tag{5.7}$$

and since $\hat{u}_t(x,\cdot) + I_{q-1}L\hat{u}(x,\cdot)$ is a polynomial of degree $q-1$

$$\zeta(x,t) = \hat{u}_t(x,t) + LI_{q-1}\hat{u}(x,t) = \sum_{j=1}^{q} \ell_j\left(\frac{t-t_n}{k_n}\right)\zeta(x,t_{nj}), \quad x \in \Omega. \tag{5.8}$$

5.3 Artificial Neural Network Representation

We approximate the solution of our problem within the neural network function space. The objective is to find $\theta^\star \in \Theta$ such that the m-th output U_m of the neural network approximates the target function $u_m(\cdot, \tilde{t}_{ni})$. Specifically, we require that the neural network output satisfies the following approximation

$$U_m(x,\tilde{t}_{ni};\theta^\star) \approx u_m(x,\tilde{t}_{ni}), \quad n = 0,\dots,N, \quad i = 1,\dots,q, \quad x \in \Omega.$$

We denote the time-space variable as $y = (x,t) \in \mathbb{R}^{d+1}$. We employ the deep residual ANN architecture proposed by Sirignano and Spiliopoulos [47]. More specifically, for a time-space input y, we define:

$$\begin{aligned}&S^0 = \tanh(W^{\text{in}}y + b^{\text{in}}),\\ &\text{DGM layer}\\ &\quad\left|\begin{aligned} G^\ell &= \tanh(V^{g,\ell}y + W^{g,\ell}S^{\ell-1} + b^{g,\ell}),\ \ell = 1,\dots,L\\ Z^\ell &= \tanh(V^{z,\ell}y + W^{z,\ell}S^{\ell-1} + b^{z,\ell}),\ \ell = 1,\dots,L\\ R^\ell &= \tanh(V^{r,\ell}y + W^{r,\ell}S^{\ell-1} + b^{r,\ell}),\ \ell = 1,\dots,L\\ H^\ell &= \tanh(V^{h,\ell}y + W^{h,\ell}(S^{\ell-1}\odot R^\ell) + b^{h,\ell}),\ \ell = 1,\dots,L\\ S^\ell &= (1-G^\ell)\odot H^\ell + Z^\ell \odot S^{\ell-1},\ \ell = 1,\dots,L\end{aligned}\right.\\ &U(y;\theta) = W^{\text{out}}S^L + b^{\text{out}},\end{aligned}$$

where L denotes the number of hidden layers and $\odot$ represents the Hadamard product. The trainable parameters θ of the model are:

$$\theta = \{W^{\text{in}}, b^{\text{in}}, (V^{\star,\ell}, W^{\star,\ell}, b^{\star,\ell})_{\ell=1,\dots,L}^{\star\in\{g,z,r,h\}}, W^{\text{out}}, b^{\text{out}}\}. \tag{5.9}$$

To train the neural network, we compute discrete approximations of the cost functional based on samples from Ω. For simplicity we consider $f = 0$; the modifications being obvious otherwise. The discrete cost functional is computed as follows:

$$\mathcal{C}_\Omega[\theta] = \frac{\text{Vol}(\Omega)}{R}\sum_{m=1}^{M}\sum_{r=1}^{R}\sum_{n=1}^{N}\int_{J_n}\zeta_m(x_r,t)^2\,\mathrm{d}t, \tag{5.10}$$

where ζ_m denotes the m-th component of ζ which is given by (5.8) and the set of points $\{x_r\}_{r=1}^R$ is generated using Sobol's low-discrepancy sequences; see, e.g., [13]. This sampling approach is more efficient for achieving a uniform coverage of the space in higher–dimensonal settings. The integral in time is computed exactly by applying integration rules which are exact for polynomials of degree $2q-2$. In the case where we have Gauss or Radau collocation points this integral is just

$$\int_{J_n} \zeta(x_r,t)^2\,\mathrm{d}t = k_n \sum_{j=1}^{q} w_j \zeta(x_r,t_{nj})^2, \tag{5.11}$$

where $w_j = \int_0^1 \ell_j(\tau)\,\mathrm{d}\tau$, and $\zeta(x,t_{nj})$ is given by (5.7).

The following are the discrete cost functionals for the initial and boundary conditions

$$\mathcal{C}_0[\theta] = \frac{\mathrm{Vol}(\Omega)}{R} \sum_{m=1}^{M}\sum_{r=1}^{R} (u_m(0,x_r;\theta) - u_{m0}(x_r))^2 \tag{5.12}$$

$$\mathcal{C}_{\partial\Omega_s}[\theta] = \frac{\mathrm{Vol}(\partial\Omega_s)}{R} \sum_{m=1}^{M}\sum_{r'=1}^{R}\sum_{n=1}^{N} (u_m(t_n,x_{r'}) - u_{ms}(x_{r'}))^2. \tag{5.13}$$

where $x_{r'}$ are Sobol points on the boundary $\partial\Omega_s$. In case we use other than Dirichlet boundary conditions, this term is modified accordingly. The deep learning approximation of the problem is characterized by the minimization of the sum of the cost functionals with respect to model parameters θ,

$$\theta^\star \leftarrow \min_{\theta\in\Theta} (\mathcal{C}_\Omega + \mathcal{C}_0 + \sum_s C_{\partial\Omega_s})[\theta]. \tag{5.14}$$

5.4 Applications

In this section we will apply our Runge–Kutta ANN schemes to heat diffusion and wave propagation initial value problems.

We will apply four alternative time–sampling approaches: three based on collocation Runge–Kutta methods and, for comparison, a uniform time–sampling scheme. Specifically, we employ the following schemes:

- Gauss: $(c_1,c_2,c_3) = \big(0.5-\sqrt{15}/10,\ 0.5,\ 0.5+\sqrt{15}/10\big)$.
- Lobatto IIIA: $(c_1,c_2,c_3) = (0,\ 0.5,\ 1)$.
- Radau IIA: $(c_1,c_2,c_3) = \big((4-\sqrt{6})/10,\ (4+\sqrt{6})/10, 1\big)$.
- Uniform Sampling.

The auxiliary modes for these collocation schemes are chosen as follows:

- Gauss and Lobatto IIIA: $(\tilde c_0,\tilde c_1,\tilde c_2,\tilde c_3) = (0, 0.25, 0.5, 1)$,
- Radau IIA: $(\tilde c_0,\tilde c_1,\tilde c_2,\tilde c_3) = \big(0, (4-\sqrt{6})/10,\ (4+\sqrt{6})/10, 1\big)$.

Notice that, in the case of Radau IIA and Lobatto IIIA methods, the points $0 = \tilde{c}_0 < \tilde{c}_1 < \tilde{c}_2 < \tilde{c}_3 = 1$ include the collocation points c_1, c_2, c_3. To ensure a fair comparison, we use four times the value of n for the uniform sampling case compared to the Runge–Kutta collocation schemes with $q = 3$.

In both of our applications, we utilized artificial neural networks as described earlier with four hidden layers, each consisting of 20 nodes. The training process employed the Adam optimizer with a learning rate of $3 \cdot 10^{-4}$. The models were trained for 20000 epochs for the heat equation and 100000 epochs for the wave equation. For the time discretization, we used 40 nodes, while the spatial grid was generated using Sobol's sequences with 256 points per epoch. These hyperparameters were carefully selected to balance computational efficiency with the accuracy of the neural network approximations of the solutions.

5.4.1 Heat Equation

We consider an initial value diffusion problem on $\Omega \in (0,1)^2$ subject to Neumann boundary conditions:

$$u_t - k(u_{xx} + u_{yy}) = 0, \quad t \in [0,1], \ (x,y) \in \Omega, \ k = 0.02, \tag{5.15}$$

$$u(x,y,0) = \left(0.5 + 0.5\cos\left(10\pi\sqrt{(x-0.6)^2 + (y-0.7)^2}\right)\right)\chi_D(x,y), \tag{5.16}$$

$$\frac{\partial u}{\partial n} = 0, \quad \text{on } \partial\Omega \times (0,1), \tag{5.17}$$

where χ_D is the characteristic function of the disk D,

$$D := \{(x,y) \in \mathbb{R}^2 : (x-0.6)^2 + (y-0.7)^2 < 0.01\}.$$

Note that the initial value is nonzero inside the disk D and zero outside D.

Fig. 5.1 shows the absolute errors at the final time $t = 1$ comparing the different schemes.

As is well known, the total heat, in the system remains conserved, i.e.,

$$\int_\Omega u(x,t)\,\mathrm{d}x = \int_\Omega u(x,0)\,\mathrm{d}x\,.$$

The conservation arises form the Neumann boundary conditions, which implies that there is no heat flow across the boundaries. In Fig. 5.2, we compare the various schemes with respect to heat conservation.

5.4.2 Heat Equation with a Discontinuous Initial Value

We replace the initial value from the previous test case with a discontinuous one. Specifically, we consider

$$u(x,y,0) = \chi_D(x,y), \tag{5.18}$$

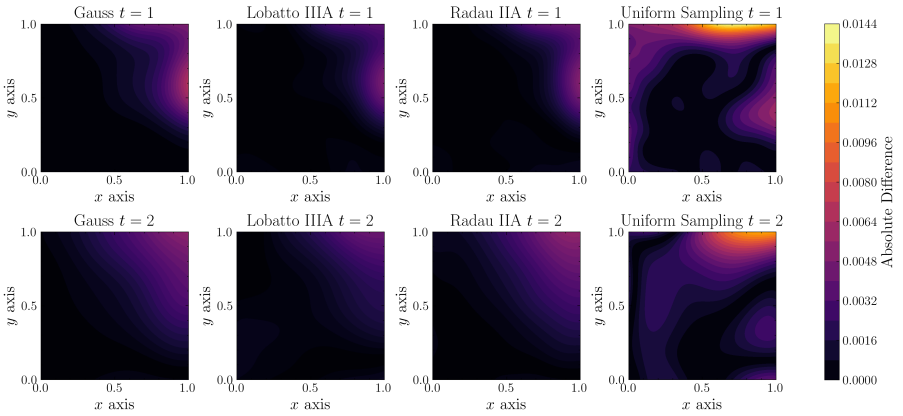

Fig. 5.1 Absolute misfit across various schemes

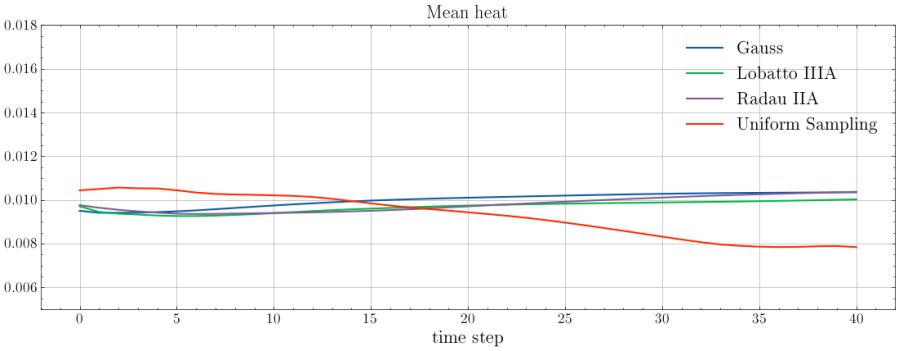

Fig. 5.2 Heat conservation (plot of $H(t) = \int_\Omega u(x,t)\,\mathrm{d}x$) across various schemes.

the characteristic function of the disk D,

$$D := \{(x,y) \in \mathbb{R}^2 : (x-0.6)^2 + (y-0.7)^2 < 0.01\}.$$

Fig. 5.3 shows the absolute errors where comparing the collocation schemes. The heat equation exhibits a notable smoothing property, which is not always maintained by various time discretization methods; see, e.g., [35], [49]. The smoothing behavior of time discretizations is a quite subtle topic, as it can influence the performance of methods when both diffusion and transport phenomena are present, particularly in the context of nonlinear PDEs and Navier–Stokes equations; see [10]. Although smoothing eventually occurs primarily due to the diffusion induced by the Quasi-Monte Carlo method used for spatial discretization, it is worth noting, as shown in Fig. 5.5, that the behavior of various discretization methods aligns with the known predictions of

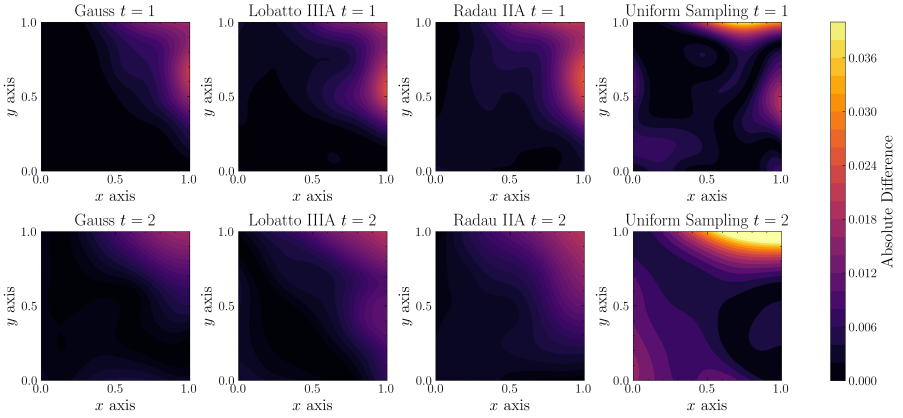

Fig. 5.3 Absolute misfit across various iterative schemes

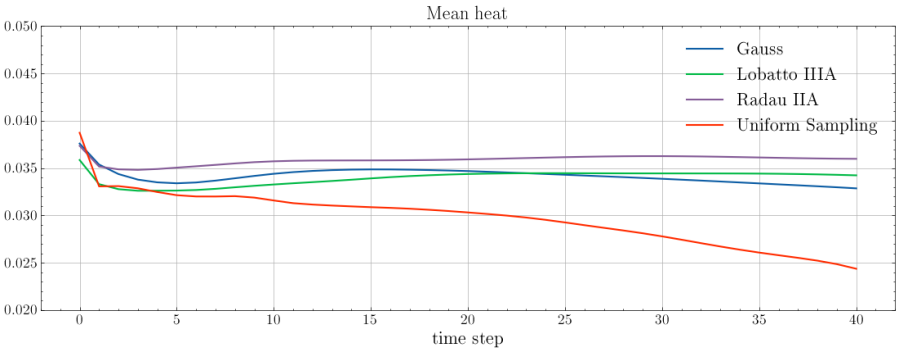

Fig. 5.4 Heat conservation across various iterative schemes.

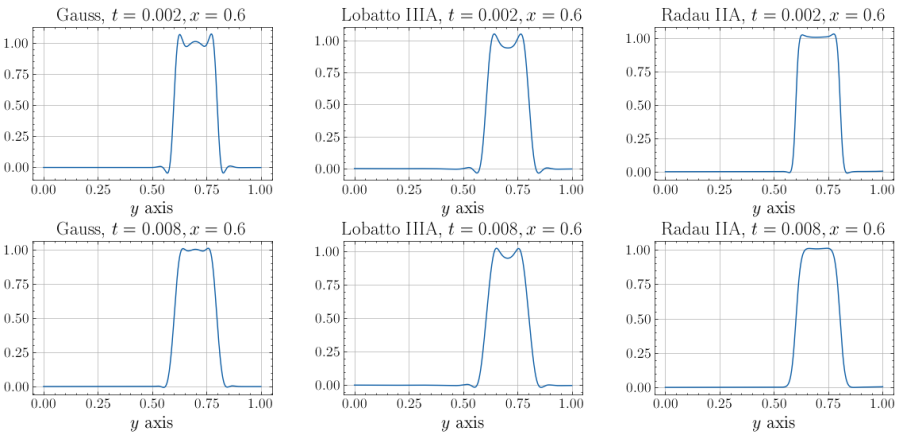

Fig. 5.5 Smoothing effect for the heat equation. As expected, Gauss and Lobatto IIIA methods have oscillating behavior close to initial times for discontinuous data. The full smoothing effect of Radau IIA methods is evident.

the corresponding Runge–Kutta schemes. In Fig. 5.4, we compare the various schemes with respect to heat conservation.

5.4.3 Wave Equation

As a third example, we consider an initial value wave propagation problem on $\Omega := (0,1)^2$ with homogeneous Dirichlet boundary conditions:

$$u_{tt} - c^2(u_{xx} + u_{yy}) = 0, \quad t \in [0,1],\ (x,y) \in \Omega,\ c = 0.5, \tag{5.19}$$

$$u(x,y,0) = \left(0.5 + 0.5\cos\left(4\pi\sqrt{(x-0.3)^2 + (y-0.5)^2}\right)\right)\chi_D(x,y), \tag{5.20}$$

$$u_t(x,y,0) = 0, \quad (x,y) \in \Omega, \tag{5.21}$$

$$u = 0, \quad \text{on } \partial\Omega \times (0,1) \tag{5.22}$$

where χ_D is the characteristic function of the disk D,

$$D := \{(x,y) \in \mathbb{R}^2 : (x-0.3)^2 + (y-0.5)^2 \leqslant 0.25^2\}.$$

As in the previous application, the support of the initial field is a closed disk.

To reformulate this as a system of first-order equations, we introduce an auxiliary variable v, representing the velocity, $v := u_t$. The corresponding system of first-order equations is given as follows:

$$\begin{pmatrix} u \\ v \end{pmatrix}_t + \begin{pmatrix} 0 & -I \\ -c^2\Delta & 0 \end{pmatrix} \begin{pmatrix} u \\ v \end{pmatrix} = \begin{pmatrix} 0 \\ 0 \end{pmatrix}, \tag{5.23}$$

where I stands for the identity operator.

For each sampling approach, Fig. 5.6 illustrates the absolute difference between the solution estimate at time $t = 1$ and the corresponding estimate delivered using the method of separation of variables, with 8 terms retained in the summation. The total energy of the system is given by

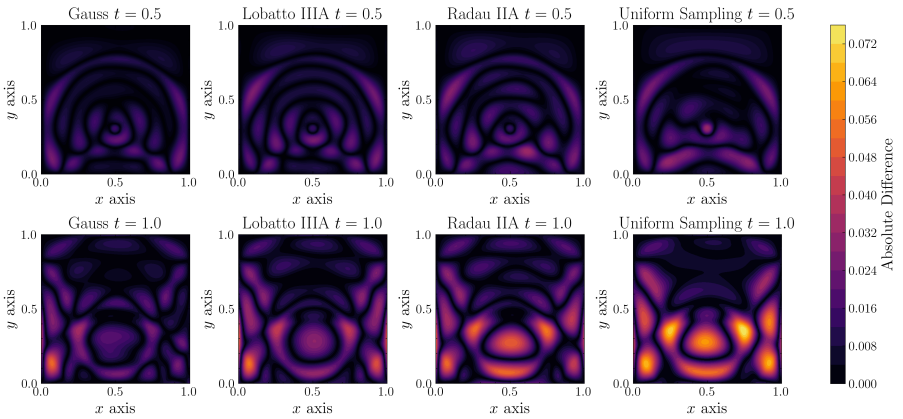

Fig. 5.6 Absolute misfit for the various iterative schemes

$$\frac{1}{2}\|u_t(t,\cdot)\|^2 + \frac{1}{2}c^2\|\nabla u(t,\cdot)\|^2 \tag{5.24}$$

with $\|\cdot\|$ the $L^2(\Omega)$-norm.

Since the total energy is conserved over time, Fig. 5.7 presents a comparison of the system's energy at each time step for the schemes under evaluation. While all methods exhibit some diffusion due to the Quasi-Monte Carlo method used for spatial discretization, it is evident that the Gauss and Lobatto IIIA methods perform as expected. These methods stand out as the optimal choice when energy conservation and high accuracy are priorities. Interestingly, the full sampling method shows the highest level of diffusive behavior.

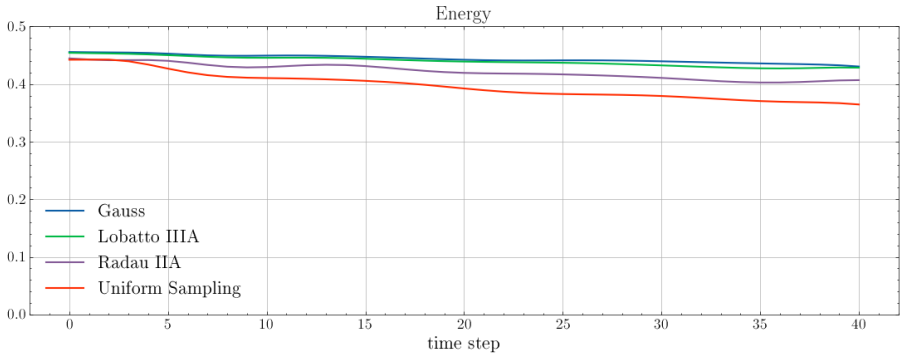

Fig. 5.7 Energy conservation across the various schemes. Gauss and Lobatto methods have superior conservation properties.

References

1. Abdeljawad, A., Grohs, Ph.: Approximations with deep neural networks in Sobolev time-space. Anal. Appl. **20**, 499–541 (2022). https://doi.org/10.1142/S0219530522500014
2. Akrivis, G., Makridakis, Ch.: On maximal regularity estimates for discontinuous Galerkin time-discrete methods. SIAM J. Numer. Anal. **60**, 180–194 (2022). https://doi.org/10.1137/20M1383781
3. Akrivis, G., Makridakis, Ch., Nochetto, R. H.: Optimal order a posteriori error estimates for a class of Runge–Kutta and Galerkin methods. Numer. Math. **114**, 133–160 (2009). https://doi.org/10.1007/s00211-009-0254-2
4. Akrivis, G., Makridakis, Ch., Nochetto, R. H.: Galerkin and Runge–Kutta methods: unified formulation, a posteriori error estimates and nodal superconvergence. Numer. Math. **118**, 429–456 (2011). https://doi.org/10.1007/s00211-011-0363-6
5. Bai, G., Koley, U., Mishra, S., Molinaro. R.: Physics informed neural networks (PINNs) for approximating nonlinear dispersive PDEs. J. Comput. Math. **39**, 816–847 (2021). https://doi.org/10.4208/jcm.2101-m2020-0342
6. Berg, J., Nyström, K.: A unified deep artificial neural network approach to partial differential equations in complex geometries. Neurocomputing **317**, 28–41 (2018). https://doi.org/10.1016/j.neucom.2018.06.056

7. Berrone, S., Canuto, C., Pintore, M.: Variational physics informed neural networks: the role of quadratures and test functions. J. Sci. Comput. **92**, 100 (2022). https://doi.org/10.1007/s10915-022-01950-4
8. Biswas, A., Tian, J., Ulusoy, S.: Error estimates for deep learning methods in fluid dynamics. Numer. Math. **151**, 753–777 (2022). https://doi.org/10.1007/s00211-022-01294-z
9. Braides, A.: Gamma-Convergence for Beginners, volume 22. Oxford Univ. Press (2002). https://doi.org/10.1093/acprof:oso/9780198507840.001.0001
10. Bristeau, M. O., Glowinski, R., Périaux, J.: Numerical methods for the Navier-Stokes equations. Applications to the simulation of compressible and incompressible viscous flows. In Finite elements in physics (Lausanne, 1986), pp. 73–187. North-Holland, Amsterdam (1987). https://doi.org/10.1007/978-3-322-87873-1
11. Butcher, J. C.: Implicit Runge-Kutta processes. Math. Comp. **18**, 50–64 (1964). https://doi.org/10.2307/2003405
12. Butcher, J. C., Wanner, G.: Runge-Kutta methods: some historical notes. Appl. Numer. Math. **22**, 113–151 (1996). Special Issue Celebrating the Centenary of Runge-Kutta Methods. https://doi.org/10.1016/S0168-9274(96)00048-7
13. Caflisch, R. E.: Monte Carlo and quasi-Monte Carlo methods. Acta Numer. **7**, 1–49. Cambridge Univ. Press, Cambridge (1998). https://doi.org/10.1017/S0962492900002804
14. Chen, X., Rosakis, Ph., Wu, Z., Zhang, Z.: Solving nonconvex energy minimization problems in martensitic phase transitions with a mesh-free deep learning approach. Comput. Methods Appl. Mech. Engrg. **416** (2023) 116384 https://doi.org/10.1016/j.cma.2023.116384
15. Crouzeix, M.: Sur les méthodes de Runge Kutta pour l'approximation des problèmes d' évolution. In *Computing methods in applied sciences and engineering (Second Internat. Sympos., Versailles, 1975), Part 1*, Vol. 134 of *Lecture Notes in Econom. and Math. Systems*, pp. 206–223. Springer, Berlin-New York (1976).
16. Crouzeix, M., Raviart, P.-A.: Approximation des équations d'évolution linéaires par des méthodes à pas multiples. *C. R. Acad. Sci. Paris Sér. A-B* **28**, Aiv, A367–A370 (1976).
17. De Giorgi, E.: Selected papers. Springer Collected Works in Mathematics. Springer, Heidelberg (2013). Editors: Ambrosio, L., Dal Maso, G., Forti, M., Miranda M., Spagnolo, S. Reprint of the 2006 edition.
18. De Ryck, T., Mishra, S., Ray, D.: On the approximation of rough functions with deep neural networks. SeMA **79**, 399–440 (2022). https://doi.org/10.1007/s40324-022-00299-w
19. Denk, R., Hieber, M., Prüss, J.: $\mathcal{R}$-boundedness, Fourier multipliers and problems of elliptic and parabolic type. Mem. Amer. Math. Soc. **166** (2003), no. 788, 114p. https://doi.org/10.1090/memo/0788
20. E, W., Yu, B.: The deep Ritz method: a deep learning-based numerical algorithm for solving variational problems. Commun. Math. Stat. **6**, 1–12 (2018). https://doi.org/10.1007/s40304-018-0127-z
21. Gazoulis, D., Gkanis, I., Makridakis, C. G.: On the stability and convergence of physics informed neural networks. IMA J. Numer. Anal. (to appear).
22. Georgoulis, E. H., Loulakis, M., Tsiourvas, A.: Discrete gradient flow approximations of high dimensional evolution partial differential equations via deep neural networks. Communications in Nonlinear Science and Numerical Simulation **117**, 106893 (2023). https://doi.org/10.1016/j.cnsns.2022.106893
23. Grekas, G., Makridakis, C. G.: Deep Ritz–Finite Element methods: Neural network methods trained with finite elements. Comput. Meth. Appl. Mech. Engng. **437**, 117798 (2025). https://doi.org/10.1016/j.cma.2025.117798
24. Grohs, P., Hornung, F., Jentzen, A., Zimmermann, P.: Space-time error estimates for deep neural network approximations for differential equations. Adv. Comput. Math. **49**, 4 (2023). https://doi.org/10.1007/s10444-022-09970-2
25. Guillou, A., Soulé, J. L.: La résolution numérique des problèmes différentiels aux conditions initiales par des méthodes de collocation. Rev. Française Informat. Recherche Opérationnelle. Série rouge **3**, 17–44 (1969). https://www.numdam.org/item/?id=M2AN_1969__3_3_17_0

26. Hairer, E., Nørsett, S. P., Wanner, G.: Solving Ordinary Differential Equations. I Non-stiff problems, vol. 8, Springer Series in Computational Mathematics. Springer-Verlag, Berlin, 2nd ed., (1993). https://doi.org/10.1007/978-3-540-78862-1
27. Hairer, E., Lubich, C., Wanner, G.: Geometric Numerical Integration: Structure-Preserving Algorithms for Ordinary Differential Equations. Springer Berlin Heidelberg, Berlin, Heidelberg (2002). https://doi.org/10.1007/3-540-30666-8
28. Kashiwabara, T., Kemmochi, T.: Discrete maximal regularity for the discontinuous Galerkin time-stepping method without logarithmic factor. SIAM J. Numer. Anal. **62**, 1638–1659 (2024). https://doi.org/10.1137/23M1580802
29. Kharazmi, E., Zhang, Z., Karniadakis, G. E.: *hp*-VPINNs: variational physics-informed neural networks with domain decomposition Comput. Methods Appl. Mech. Engrg. **374**, 113547 (2021). https://doi.org/10.1016/j.cma.2020.113547
30. Kovács, B., Li, B., Lubich, C.: A-stable time discretizations preserve maximal parabolic regularity. SIAM J. Numer. Anal. **54**, 3600–3624 (2016). doi: 10.1137/15M1040918
31. Kunstmann, P. C., Weis, L.: Maximal L_p-regularity for Parabolic Equations, Fourier Multiplier Theorems and H^∞-functional Calculus. Functional Analytic Methods for Evolution Equations. Lect. Notes Math. **1855**, 65–311 (2004). doi: 10.1007/978-3-540-44653-8_2
32. Lagaris, I.E., Likas, A., Fotiadis, D.I.: Artificial neural networks for solving ordinary and partial differential equations. *IEEE Transactions on Neural Networks* **9**, 987–1000 (1998). https://doi.org/10.1109/72.712178
33. Leykekhman, D., Vexler, B.: Discrete maximal parabolic regularity for Galerkin finite element methods. Numer. Math. **135**, 923–952 (2017). https://doi.org/10.1007/s00211-006-0821-2
34. Loulakis, M., Makridakis, Ch. G.: A new approach to generalisation error of machine learning algorithms: Estimates and convergence. arXiv2306.13784 (2023). https://arxiv.org/abs/2306.13784
35. Luskin, M., Rannacher, R.: On the smoothing property of the Crank-Nicolson scheme. Applicable Anal. **14**, 117–135 (1982/83). https://doi.org/10.1080/00036818208839415
36. Makridakis, Ch., Nochetto, R. H.: A posteriori error analysis for higher order dissipative methods for evolution problems. Numer. Math. **104**, 489–514 (2006). https://doi.org/10.1007/s00211-006-0013-6
37. Makridakis, Ch. G., Pim, A., Pryer, T.: A deep Uzawa-Lagrange multiplier approach for boundary conditions in PINNs and deep Ritz methods. Journal of Machine Learning (to appear).
38. Makridakis, Ch. G., Pim, A., Pryer, T.: Deep Uzawa for PDE constrained optimisation. arXiv2410.17359 (2024). https://arxiv.org/abs/2410.17359
39. Mishra, S., Molinaro, R.: Estimates on the generalization error of physics-informed neural networks for approximating a class of inverse problems for PDEs. IMA J. Numer. Anal. **42**, 981–1022 (2022). https://doi.org/10.1093/imanum/drab032
40. Mishra, S., Molinaro, R.: Estimates on the generalization error of physics-informed neural networks for approximating PDEs. IMA J. Numer. Anal. **43**, 1–43 (2023). https://doi.org/10.1093/imanum/drab093
41. Müller, J., Zeinhofer, M.: Deep Ritz revisited. arXiv:1912.03937 https://arxiv.org/abs/1912.03937 (2019). ICLR Workshop on Integration of Deep Neural Models and Differential Equations (2020).
42. Raissi, M., Karniadakis, G. E.: Hidden physics models: Machine learning of nonlinear partial differential equations. J. Comput. Phys. **357**, 125–141 (2018). https://doi.org/10.1016/j.jcp.2017.11.039
43. Raissi, M., Perdikaris, P., Karniadakis, G. E.: Physics-informed neural networks: a deep learning framework for solving forward and inverse problems involving nonlinear partial differential equations. J. Comput. Phys. **378**, 686–707 (2019). https://doi.org/10.1016/j.jcp.2018.10.045
44. Rico-Martinez, R., Krischer, K., Kevrekidis, I.G., Kube, M.C., and Hudson, J.L.: Discrete-vs. continuous-time nonlinear signal processing of Cu electrodissolution data. Chemical Engineering Communications **118**, 25–48 (1992). https://doi.org/10.1080/00986449208936084

45. Shin, Y., Darbon, J., Karniadakis, G. E.: On the convergence of physics informed neural networks for linear second-order elliptic and parabolic type PDEs. Commun. Comput. Phys. **28**, 2042–2074 (2020). https://doi.org/10.4208/cicp.OA-2020-0193
46. Shin, Y., Zhang, Z., Karniadakis G. E.: Error estimates of residual minimization using neural networks for linear pdes. Journal of Machine Learning for Modeling and Computing **4**, 73-101 (2023). https://doi.org/10.1615/JMachLearnModelComput.2023050411
47. Sirignano, J., Spiliopoulos, K.: DGM: a deep learning algorithm for solving partial differential equations. J. Comput. Phys. **375**, 1339–1364 (2018). https://doi.org/10.1016/j.jcp.2018.08.029
48. Sukumar, N., Srivastava, A.: Exact imposition of boundary conditions with distance functions in physics-informed deep neural networks. Comput. Meth. Appl. Mech. Engng. **389**, 114333 (2022). https://doi.org/10.1016/j.cma.2021.114333
49. Thomée, V.: Galerkin Finite Element Methods for Parabolic Problems. 2nd ed., Springer–Verlag, Berlin (2006). https://doi.org/10.1007/3-540-33122-0
50. Wright, K.: Some relationships between implicit Runge-Kutta, collocation Lanczos τ methods, and their stability properties. BIT **10**, 217–227 (1970). https://doi.org/10.1007/BF01936868
51. Xu, J.: Finite neuron method and convergence analysis. Commun. Comput. Phys. **28**, 1707–1745 (2020). https://doi.org/10.4208/cicp.OA-2020-0191
52. Zheng, S.: Nonlinear Evolution Equations. Chapman and Hall/CRC (2004). https://doi.org/10.1201/9780203492222